NeuroImage 51 (2010) 1319–1333

Contents lists available at ScienceDirect

NeuroImage

journal homepage: www.elsevier.com/locate/ynimg

Identifying robust and sensitive frequency bands for interrogating neural oscillations

Alexander J. Shackman [a,*,1], Brenton W. McMenamin [b,*,1], Jeffrey S. Maxwell [c], Lawrence L. Greischar [d], Richard J. Davidson [e,*]

[a] Wisconsin Psychiatric Institute and Clinics, Departments of Psychology and Psychiatry, University of Wisconsin-Madison, WI, USA
[b] Center for Cognitive Sciences and Department of Psychology, University of Minnesota-Twin Cities, MN, USA
[c] U.S. Army Research Laboratory, Aberdeen, MD; Laboratory for Affective Neuroscience, University of Wisconsin-Madison, WI, USA
[d] Laboratory for Affective Neuroscience and Waisman Laboratory for Brain Imaging and Behavior, University of Wisconsin-Madison, WI, USA
[e] Laboratory for Affective Neuroscience, Waisman Laboratory for Brain Imaging and Behavior, HealthEmotions Research Institute, and Center for Investigating Healthy Minds, Departments of Psychology and Psychiatry, University of Wisconsin-Madison, WI, USA

ARTICLE INFO

Article history:
Received 4 December 2009
Revised 7 March 2010
Accepted 11 March 2010
Available online 18 March 2010

ABSTRACT

Recent years have seen an explosion of interest in using neural oscillations to characterize the mechanisms supporting cognition and emotion. Oftentimes, oscillatory activity is indexed by mean power density in predefined frequency bands. Some investigators use broad bands originally defined by prominent surface features of the spectrum. Others rely on narrower bands originally defined by spectral factor analysis (SFA). Presently, the robustness and sensitivity of these competing band definitions remains unclear. Here, a Monte Carlo-based SFA strategy was used to decompose the tonic ("resting" or "spontaneous") electroencephalogram (EEG) into five bands: *delta* (1–5 Hz), *alpha-low* (6–9 Hz), *alpha-high* (10–11 Hz), *beta* (12–19 Hz), and *gamma* (>21 Hz). This pattern was consistent across SFA methods, artifact correction/rejection procedures, scalp regions, and samples. Subsequent analyses revealed that SFA failed to deliver enhanced sensitivity; narrow alpha sub-bands proved no more sensitive than the classical broadband to individual differences in temperament or mean differences in task-induced activation. Other analyses suggested that residual ocular and muscular artifact was the dominant source of activity during quiescence in the delta and gamma bands. This was observed following threshold-based artifact rejection or independent component analysis (ICA)-based artifact correction, indicating that such procedures do not necessarily confer adequate protection. Collectively, these findings highlight the limitations of several commonly used EEG procedures and underscore the necessity of routinely performing exploratory data analyses, particularly data visualization, prior to hypothesis testing. They also suggest the potential benefits of using techniques other than SFA for interrogating high-dimensional EEG datasets in the frequency or time–frequency (event-related spectral perturbation, event-related synchronization/desynchronization) domains.

Recent years have witnessed a renewed interest in using spectral indices of electroencephalographic (EEG) activity, that is, neural oscillations, to characterize the neural mechanisms supporting cognition and emotion in health and disease (e.g., Uhlhaas and Singer, 2010). Oftentimes, this oscillatory activity is indexed by power in *a priori* frequency bands. This is particularly true for studies of the tonic (i.e., resting or spontaneous) EEG. Some investigators use relatively broad bands (e.g., alpha: 8–13 Hz) that were originally defined on the basis of key surface features, such as the average peak frequency. Others favor narrower bands (e.g., alpha-1: 8–10 Hz; alpha-2: 11–13 Hz) that were originally identified using spectral factor analysis (SFA). Despite the widespread application of both kinds of bands, two fundamental questions remain unanswered. First, are the narrow bands defined by SFA of the tonic EEG robust or are they strongly dependent on the manner in which SFA is implemented? Second, do the broad and narrow bands differ in their sensitivity? The major aim of the present study was to answer these questions, with a special emphasis on the alpha band, using a novel combination of psychometric and electrophysiological techniques.

Activity in the alpha band is among the most prominent features of the electroencephalogram (EEG) in both the time- and frequency-domains (Fig. 1). Moreover, its intermediate position in the spectrum renders it less susceptible to common artifacts than the other frequency bands (delta: 1–4 Hz; theta: 4–8 Hz; beta: 14–30 Hz; gamma, >30 Hz; Niedermeyer, 2005). Such artifacts include both low-frequency ocular and high-frequency myogenic activity (Shackman et al., 2009b). Given these virtues, it is not surprising that alpha has

* Corresponding authors. University of Wisconsin-Madison, 1202 West Johnson Street, Madison, WI 53706, USA.
E-mail addresses: shackman@wisc.edu (A.J. Shackman), mcmen020@umn.edu (B.W. McMenamin), rjdavids@wisc.edu (R.J. Davidson).
[1] Alexander Shackman and Brenton McMenamin are co-first authors.

1053-8119/$ – see front matter © 2010 Elsevier Inc. All rights reserved.
doi:10.1016/j.neuroimage.2010.03.037

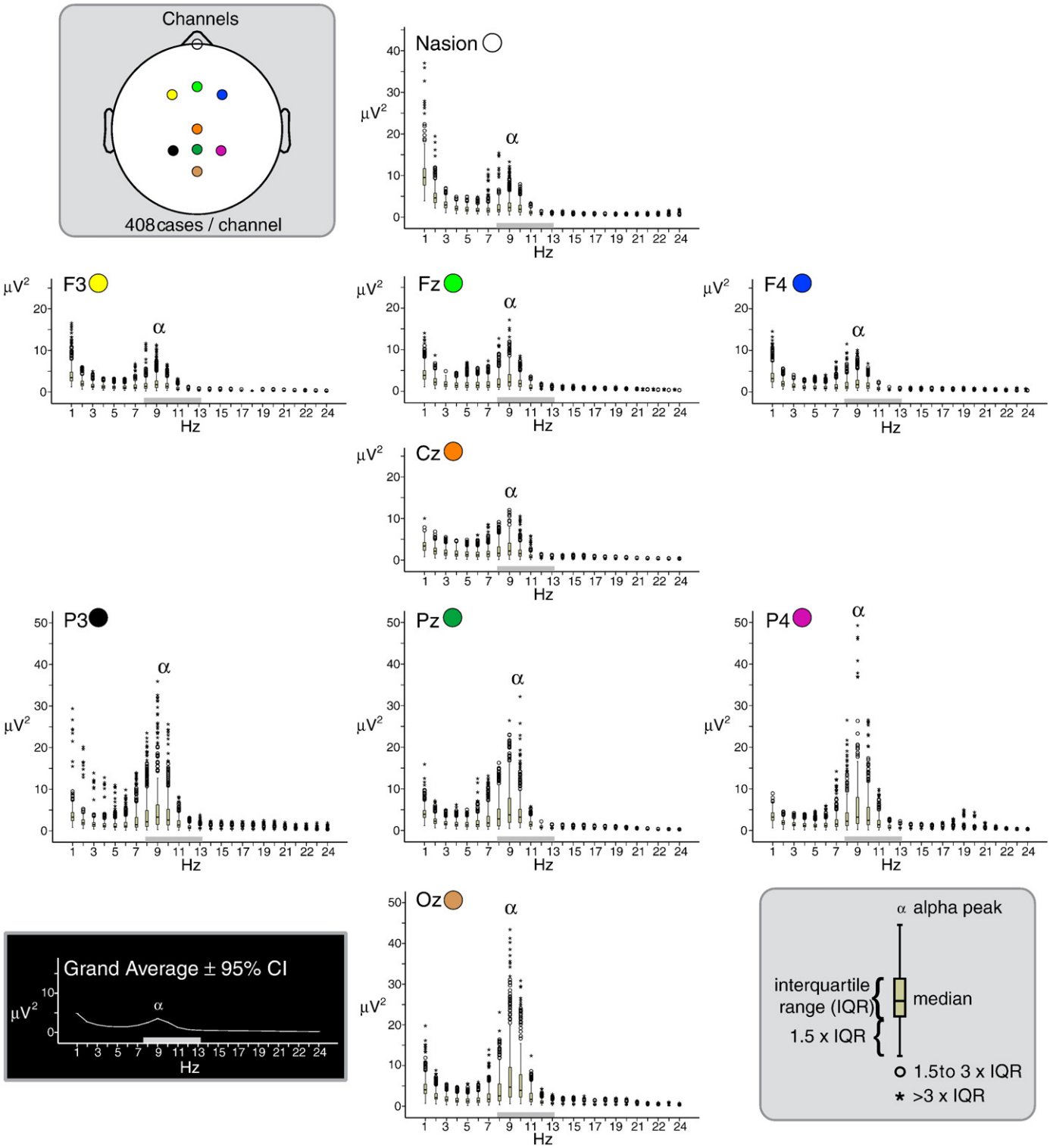

Fig. 1. Power spectra for the primary sample ($n = 51$). Box-plots depict the median power (μV^2) at each frequency, rounded to the nearest integer, at representative electrodes for the average reference. Error bars (i.e., whiskers) indicate the variability across participants and blocks ($51 \times 8 = 408$ cases per frequency), indexed by the interquartile range (IQR; 25th–75th percentile). Gray bar along the *x*-axis indicates the limits of the classical alpha band (8–13 Hz). Grand average (lower left) depicts the mean power (±95% CI) at each frequency. Values are based on the complete data matrix submitted to the whole-scalp SFA, comprising channels, participants, and blocks ($129 \times 51 \times 8 = 52{,}632$ cases per frequency). Approximate locations of each channel on the scalp (coded by color) are depicted at the upper left.

been among the most widely employed EEG metrics in the frequency-domain, from early research (Berger, 1929/1969), to recent studies of cognition (Freunberger et al., 2009; Hamidi et al., 2009), emotion (Carver and Harmon-Jones, 2009; Shackman et al., 2009a), and psychopathology (Thibodeau et al., 2006).

Much of this research has quantified alpha activity as mean power spectral density (μV^2/Hz) in a broad band ranging from 8 to 13 Hz. This convention, and those defining the other classical EEG bands, was established on the basis of expert consensus about its key distinguishing characteristics (Brazier et al., 1961). For the alpha rhythm, early

work suggested that these include a mean frequency of ~10 Hz (SD = ~1 Hz), peak amplitude at midline parieto-occipital electrodes, and topographically specific suppression (i.e., desynchronization or blocking) in response to attention-demanding tasks (Niedermeyer, 2005; Shaw, 2003). More recent studies employing high-density electrode arrays and Fourier analyses have confirmed these generalizations (Aurlien et al., 2004; Clark et al., 2004; Marcuse et al., 2008; Tenke and Kayser, 2005; van Albada et al., 2010). Consequently, the conventional broadband definition of alpha has remained largely unchanged for nearly 50 years (Nuwer et al., 1999). But whether this definition represented the optimal measure of "alpha-like" brain electrical activity or the most sensitive index of the psychological processes instantiated in that activity remains unclear (Andresen, 1993; Buzsaki, 2006).

SFA represents a prominent alternative technique for defining spectral bands (Andresen, 1993). SFA entails three conceptually distinct steps (see the Supplement). First, principal components analysis (PCA) or related techniques are used to extract factors (i.e., orthogonal, weighted combinations of variables) from the correlation or covariance matrix formed by the power at each measured frequency. Second, factors that are ill defined or account for little variance are discarded (Zwick and Velicer, 1986). Third, frequency bands are defined by rotating and then thresholding the loadings (i.e., weights) for the remaining factors.

Early SFA research suggested that the classical alpha band is divisible into two relatively narrow sub-bands, alpha-low and alpha-high (Andresen, 1993; Kubicki et al., 1979; Mecklinger et al., 1992). This conclusion continues to exert an enormous impact on contemporary research on neural oscillations. For instance, the International Federation of Clinical Physiology now has an explicit provision for such sub-bands (Nuwer et al., 1999). Likewise, the widely used LORETA-Key source modeling package (http://www.uzh.ch/keyinst/loreta) makes use of alpha sub-bands (Pascual-Marqui et al., 1999). Moreover, numerous contemporary studies of the tonic EEG (Davidson et al., 2000b; Shackman et al., 2009a), EEG coherence (Nunez et al., 2001), task-induced EEG activity (Gevins et al., 1997; Neuper and Pfurtscheller, 2001; Nunez et al., 2001; Wacker et al., 2003), and drug-induced changes in the EEG (Knott, 2001) have relied on alpha sub-bands that were pre-defined on the basis of SFAs performed on independent samples of the tonic EEG. Such *a priori* sub-bands have also been used in concurrent EEG-neuroimaging studies (Jann et al., 2009; Oakes et al., 2004; Pizzagalli et al., 2004; Ritter et al., 2009) and recommended for routine use in psychiatric investigations (Boutros et al., 2008).

But it remains unclear whether the bands defined by SFA are sufficiently robust to warrant such generalization. This ambiguity stems from several key limitations of prior SFA studies (Andresen, 1993; Arruda et al., 1996). First, many early investigations employed samples of convenience that were too small to ensure robustness or too idiosyncratic to ensure generality (Guadagnoli and Velicer, 1988). Second, all of the early SFA studies used data from four or fewer channels clustered over posterior or central locations. Consequently, their applicability to other regions of the scalp or high-resolution electrode arrays is unresolved. Third, many studies used measures of relative spectral power, introducing artificial algebraic dependencies into the data (Comrey and Lee, 1992), or extracted factors from the covariance matrix. Use of the covariance matrix is problematic because it weights the solution in favor of high-variance electrodes and frequencies (Arruda et al., 1996). When SFA is performed on the tonic EEG, the resulting band definitions will necessarily emphasize the contribution of posterior channels and frequencies in the alpha range. This is depicted in Fig. 1, which underscores the much greater variability (i.e., interquartile range), of the posterior alpha peak compared to the remainder of the scalp and spectrum. Fourth, most studies employed factor retention criteria (e.g., cumulative variance threshold, Scree plot, Kaiser-Guttman criterion) that are now widely considered unreliable (Peres-Neto et al., 2005; Velicer et al., 2000). Retaining too few factors can lead to the artificial fusion of bands (Fava and Velicer, 1996). Conversely, retaining too many factors can produce artificial splitting, creating narrow bands at the expense of broader genuine ones (Lawrence and Hancock, 1999; Wood et al., 1996). Contemporary SFA investigations suffer from many of the same problems (e.g., Debener et al., 2000; Duffy et al., 1992; Goncharova and Davidson, 1995; Tenke and Kayser, 2005).

The impact of using SFA-defined bands on sensitivity also remains unresolved. A key motivation for using SFA-defined bands is the possibility of enhancing sensitivity (i.e., using the covariance structure of the spectrum to separate oscillations that would otherwise be averaged together). But there is nothing inherent in the mathematics of SFA to guarantee that the dimensions it identifies correspond to the most psychophysiologically informative or statistically sensitive bases (Donchin and Heffley, 1978; Lobaugh et al., 2001).

The existing empirical record does not resolve the issue of differential sensitivity. Some studies have provided evidence that narrowly defined alpha sub-bands exhibit psychologically and topographically distinct changes in *task-induced* activity (Gevins et al., 1997; Klimesch, 1999; Niedermeyer, 2005; Nunez et al., 2001). Likewise, several studies have suggested that alpha-low is more sensitive than alpha-high to experimental manipulations of mood (state affect; Crawford et al., 1996; Davidson et al., 2000b; Everhart and Demaree, 2003; Everhart et al., 2003; Wacker et al., 2003). Along similar lines, *tonic activity* in the alpha-low band seems to be more sensitive to individual differences in temperament (trait affect; Goncharova and Davidson, 1995). Nevertheless, inconsistencies and null results have been reported (Crawford et al., 1996; Everhart et al., 2008; Papousek and Schulter, 2001; Wyczesany et al., 2008). In particular, the upper and lower alpha sub-bands have been found to exhibit virtually identical heritability (Smit et al., 2005), relations with tonic thalamic glucose metabolism (Larson et al., 1998), and intracerebral sources (Babiloni et al., 2009). This ambiguity is compounded by the fact that the sensitivity of alpha-low and alpha-high was not directly compared in the vast majority of these studies. And, to our knowledge, no study has examined whether using alpha sub-bands identified on the basis of SFA of the *tonic* EEG alters sensitivity to *task-induced* oscillations.

The aim of the present investigation was to examine the robustness and sensitivity of SFA-defined frequency bands using methods designed to circumvent these limitations. Factors were first extracted from a high-resolution tonic EEG dataset using the correlation matrix. Factor retention was determined using a Monte Carlo technique ("parallel analysis;" Horn, 1965; Velicer et al., 2000). Robustness was assessed by comparing SFA-defined alpha bands across variations in SFA methodology (e.g., choice of rotation) and regions of the scalp (for a similar approach, see Freeman and Grajski, 1987).

The sensitivity of the alpha sub-bands to individual differences in tonic activity and mean differences in task-induced oscillatory activity was also assessed. Individual differences analyses took advantage of a large body of data showing that more anxious, behaviorally inhibited individuals tend to show lateralized reductions in tonic alpha power at right mid-frontal electrodes (Shackman et al., 2009a).[2] Accordingly, correlations were computed between EEG asymmetry (i.e., laterality) scores computed for the mid-frontal electrodes and scores on the Behavioral Inhibition System questionnaire (BIS; Carver and White, 1994), a commonly used measure of anxious temperament (Carver et al., 2000; Elliot and Thrash, 2002). Mean differences analyses

[2] Individuals with greater right-frontal activity are predisposed to experience more intense negative affect when challenged by aversive stimuli (Tomarken et al., 1990; Wheeler et al., 1993) and rate themselves as more extreme on measures of trait anxiety (Blackhart et al., 2006; Mathersul et al., 2008; Petruzzello and Landers, 1994; Tomarken and Davidson, 1994), anxious arousal (Mathersul et al., 2008; Stewart et al., 2008), negative affectivity (Jacobs and Snyder, 1996; Tomarken et al., 1992a), and behavioral inhibition (Shackman et al., 2009a; Sutton and Davidson, 1997). Similar relations have been obtained in nonhuman primates and children (Buss et al., 2003).

exploited the robust reduction in alpha power that typically occurs at posterior midline channels in response to opening the eyes (Berger, 1929/1969; Niedermeyer, 2005). For both kinds of sensitivity analysis, SFA-defined sub-bands were compared to one another and to conventional alpha bands. This included the broadband alpha range (8–13 Hz) and narrow *a priori* sub-bands (alpha-low: 8–10 Hz; alpha-high: 11–13 Hz; e.g., Shackman et al., 2009a).

Method

Participants

Participants were obtained from two previously published samples. In both cases, individuals were recruited from the University of Wisconsin-Madison community and paid $10/h. Participants provided informed consent in accord with guidelines established by the local Institutional Review Board.

Primary sample

Most analyses employed the sample described in Shackman et al. (2009a). This comprised 51 right-handed females (M = 19.5 years, SD = 1.9) recruited as part of a larger program of research on neurobiological indices of temperament.

Secondary sample

Analyses of mean differences in task-induced activation employed the smaller sample described in McMenamin et al. (2010, 2009). This consisted of 17 individuals (16 female; M = 24.1 years, SD = 7.1).

Procedures

Primary sample

Participants came to the laboratory on two occasions separated by several weeks. In the first session, participants provided consent and completed the BIS (see the Supplement). During the second session, sensors were applied shortly after arrival. After ensuring adequate data quality (30–45 min), four or eight 60-s blocks of tonic EEG (half eyes-open/closed; order counterbalanced) were acquired. No attempt was made to systematically record the condition for each block, given that the eyes-open/-closed distinction is typically ignored in EEG studies of temperament (e.g., Tomarken et al., 1992a).

Secondary sample

Procedures were similar, although analog event-markers were used to mark each block with the appropriate condition and participants came to the laboratory for only a single session. Measures of temperament were not collected. EEG was acquired during eight 32-s blocks (half eyes-open/closed; order counterbalanced; four blocks/condition). Participants were instructed to remain relaxed throughout each block.

EEG acquisition and pre-processing

Procedures were identical to those detailed in our prior reports (McMenamin et al., 2010; Shackman et al., 2009a). EEG was acquired using a 128-channel montage (http://www.egi.com) referenced to Cz, filtered (0.1–200 Hz), amplified, and digitized (500 Hz). Using EEGLAB (http://sccn.ucsd.edu/eeglab) and in-house code written for Matlab (http://www.mathworks.com), calibrated (μV) data were filtered (60-Hz).

For the primary sample, a conventional artifact rejection procedure was employed (Delorme et al., 2007a). Specifically, epochs (1.024-s) contaminated by gross artifacts (±100 μV for more than half an epoch or $\sigma^2 > 500$) or flat channels ($\sigma^2 < 0.25\ \mu V^2$) were rejected (median number of epochs retained = 435.0, SD = 216.8).

For the secondary sample, independent component analysis (ICA) was used to attenuate artifact. In this case, bad channels (±100 μV for >20 s) and gross artifacts (±100 μV for >4 channels) were manually identified and rejected. A 0.5 Hz high-pass filter was used to attenuate channel drift and satisfy ICA's stationarity assumption (Onton et al., 2006). Consistent with other high-resolution EEG studies (Delorme et al., 2007b), spatial Principal Components Analysis (PCA) was used to reduce the dimensionality of the EEG from 128 channels to 64 principal components (PCs) prior to performing extended Infomax ICA (Bell and Sejnowski, 1995; Lee et al., 1999). Components were classified by two raters. Inter-rater reliability, indexed using Krippendorff's alpha (Hayes and Krippendorff, 2007), was excellent, $\alpha = .98$. Components containing gross (e.g., reference, ground, electrocardiographic, and line), ocular, or frank electromyographic (EMG) artifacts were rejected. Following reconstruction of the filtered time-series, epochs with residual artifact (i.e., deviations exceeding ±200 μV for more than half an epoch or variance exceeding 1000 μV^2) or flat channels (epoch variance less than 0.25 μV^2) were automatically rejected.

For both samples, rejected channels were interpolated with a spherical spline when at least one neighboring electrode was usable (Greischar et al., 2004). "Artifact-free" data were re-referenced to an average montage. When adequate spatial sampling of the scalp is achieved, as in the present experiment, an average reference montage is least biased and most reliable (Davidson et al., 2000a; Dien, 1998; Gudmundsson et al., 2007). Mean power spectral (μV^2) was estimated for each frequency (0–48.83 Hz; 0.98 Hz/bin nominal resolution) using 50% overlapped, sliding Hann-tapered epochs (Welch, 1967). Fourier procedures were checked using a 10 Hz sine wave digital calibration file. For the primary sample, artifact-free epochs were randomly sorted into eight equal-length blocks/participant. For the secondary sample, blocks were collapsed according to condition (eyes-open vs. -closed). A similar number of artifact-free epochs were retained for the eyes-open (Median = 242; SD = 4.1) and -closed (Median = 244; SD = 5.1) conditions, $p = .37$.

SFA

Overview of robustness assessment

Three kinds of robustness were examined. *Anatomical invariance* was assessed by dividing the electrode array into quadrants and comparing the solutions yielded by each. *Extraction stability* was assessed by comparing solutions differing in the number of factors retained (i.e., ±1 from the number determined by Monte Carlo). *Rotational stability* was assessed by comparing orthogonal and oblique rotations. Although most prior work has relied on orthogonal rotations, some have argued that oblique rotations (e.g., promax), in which factors are allowed to correlate, are more physiologically plausible (Andresen, 1993; Dien, 2010; Dien et al., 2005). The band definitions produced by orthogonal rotation of the complete montage (Tenke and Kayser, 2005), with factor retention determined by Monte Carlo, were treated as the primary SFA.

Factor extraction

For the primary SFA, the inter-frequency correlation matrix was generated using the 50-bin spectra (0.98–48.83 Hz) for each combination of channel, block, and participant ($129 \times 8 \times 51 = 52{,}632$ cases). Following prior recommendations, this matrix was generated for data in units of μV^2, rather than $\log_{10}\mu V^2$ (Ferree et al., 2009; Tenke and Kayser, 2005). For tests of *anatomical invariance*, this was computed separately for each of four overlapping regions of interest (ROIs) on the scalp (38 channels/region: left, right, anterior, posterior). Channels along the edge of the array were intentionally excluded from the ROIs to allow us to ascertain their impact on the SFA solution. Some prior work suggests that such channels are particularly vulnerable to residual artifact (McMenamin et al., 2010). In all cases, 50 factors (i.e., principal components) were initially extracted using SPSS version 16.0.1 (http://www.spss.com).

Factor retention

Factor retention was determined using Matlab code implementing parallel analysis (http://people.ok.ubc.ca/brioconn/nfactors/nfactors.html), a variant of the Kaiser-Guttman criterion (eigenvalue >1) that explicitly accounts for sampling error (Horn, 1965; Velicer et al., 2000). Specifically, a Monte Carlo approach is used to generate confidence intervals for the null distribution of eigenvalues. Here, we generated 1000 random data matrices with dimensions paralleling those of the observed data matrix (52,632 cases × 50 frequency-bins). Next, correlation matrices were computed and PCA was used to extract eigenvalues from each. These were used to compute 95th percentile confidence intervals (CI). For our primary analyses, factors were retained when the *i*th observed eigenvalue exceeded the CI for the corresponding rank in the simulated null distribution.

Factor rotation and post-processing

Retained factors were rotated using SPSS. Final bands were formed on the basis of bins with loadings ≥.60, a value conventionally described as "good" to "very good" (Comrey and Lee, 1992). The rationale for this choice is detailed in the Supplement.

Analytic strategy for individual differences analyses

The aim of inferential tests was to assess whether SFA-defined alpha sub-bands differed from one another or conventionally defined alpha (sub-)bands in their sensitivity to individual differences in the BIS. Accordingly, mean power density estimates were $\log_{10}$-transformed to normalize the distribution (Gasser et al., 1982) and asymmetry scores were computed by subtracting the left-hemisphere sensor from the right-hemisphere sensor for homologous electrodes. Reductions in power were interpreted as greater cerebral activity. Consequently, negative asymmetry scores indicated less left- than right-hemisphere activity (or, equivalently, more right- than left-hemisphere activity). Analyses employed permutation-based non-parametric tests written in MATLAB (http://www.themathworks.com). For each, 10,000 permutations were conducted.

Multiple regressions were used to test whether individual differences in BIS sensitivity predicted asymmetries on the scalp overlying PFC. BAS was included as a simultaneous predictor to ensure specificity. Correlations are reported as semi-partial coefficients. Uncorrected *p*-values for each electrode-pair were estimated via permutation (ter Braak, 1992). The predictor of interest (BIS) was randomly permuted—while the values of the covariate (BAS) were fixed—to generate a coefficient-distribution at each electrode. The values demarcating the upper/lower 2.5th percentiles were used as the uncorrected *p*-values. To minimize the number of comparisons, analyses were restricted *a priori* (cf. Sutton and Davidson, 1997) to the mid- (F3/4) and lateral-frontal electrodes (F7/8) and their nearest neighbors (12 electrode-pairs total). Correction for multiple comparisons was performed using a minimum-*p* technique (Nichols and Holmes, 2002). At electrodes exhibiting a significant regression, pairwise tests (Hotelling, 1940) were used to test whether bands differed in their association with the BIS.

Results

Descriptive statistics for spectra

Spectra for representative channels are depicted in Fig. 1. Results were consistent with prior studies using similar methodology and sample demographics (Chen et al., 2008, 2006; Tenke and Kayser, 2005; Van Albada et al., 2007). Power in the alpha range (8–13 Hz) peaked at 9 Hz across the scalp. The mean and variance of broadband alpha power peaked at bilateral parieto-occipital electrodes (peak: PO1, 5.2 μV^2/Hz). Qualitatively, the two slopes of the alpha peak were asymmetric, with a sharper decline on the high-frequency side. This is consistent with prior reports as well (Klimesch, 1999). Median power in the delta range (1–4 Hz) was maximal at frontopolar and anterofrontal sites bordering the face and eyes. A distinct peak was not observed for power in the classical theta range (4–8 Hz).

The correlation matrix for the lower frequencies used in the primary SFA is presented in Supplementary Table 2. There was substantial heterogeneity in the magnitude of the correlations among frequencies constituting the classical alpha band (M = .58, SD = .17); several were quite modest in size (range: .37–.89). The internal-consistency of the alpha band, indexed by computing Cronbach's coefficient α (Cortina, 1993; Nunnally and Bernstein, 1994) across frequencies, was approximately .70 (see the Supplement). Taken with the mean inter-frequency correlation, this value is sufficiently low to suggest that the classical alpha band might be multidimensional, that is, divisible into narrower sub-bands (Cortina, 1993).

SFA

The results of the primary SFA are detailed in Table 1. The whole-scalp SFA—employing Monte Carlo-based factor retention and varimax factor rotation—yielded five factors, collectively accounting for 89.3% of the variance in the spectrum. Consistent with the inter-frequency correlations (Supplementary Table 2), thresholding the rotated factor loadings yielded the following SFA-defined bands: delta (range: 1–5 Hz; peak: 2 Hz), alpha-low (range: 6–9 Hz; peak: 8 Hz), alpha-high (range: 10–11 Hz; peak: 10 Hz), beta (range: 12–19 Hz; peak: 14 Hz), and gamma (range: 21–49 Hz; peak: 40 Hz). These are depicted in Fig. 2. Correlations among conventional and SFA-defined alpha bands are presented in Supplementary Table 3. Collapsed over electrodes, the correlation among SFA-defined alpha sub-bands was moderate, $r = .38$, $p = .006$. The narrow range of SFA-defined alpha-high is consistent with prior observations (Klimesch, 1999).[3] A frank theta band was not identified. Reliability estimates for the SFA-defined bands are presented in Supplementary Table 1.

Spline-interpolated topographic plots of power density for each of the SFA-defined bands are depicted in Fig. 3. Several features warrant comment. First, the band topographies were grossly symmetric and consistent with prior high-resolution EEG studies (Chen et al., 2008, 2006; Jann et al., 2009; Lehmann, 1971). Second, power in both the low-frequency delta and high-frequency gamma bands was maximal at frontopolar and anterofrontal electrodes in the vicinity of the face and eyes. This suggests that the dominant source of activity in these bands was likely artifactual, presumably arising from a combination of residual ocular, myogenic and movement artifacts. A similar pattern, albeit markedly smaller in amplitude, was visible in the adjacent alpha-low and beta bands. Third, the alpha-low, alpha-high, and beta bands were all characterized by similar topographies with maximal power at bilateral parieto-occipital electrodes. Peak power in the beta band was much lower than the alpha bands, suggesting that the posterior "hot spots" characterizing beta might represent roll-off from the adjacent alpha peak (Figs. 2 and 3). The strong topographic resemblance of the three narrow bands (alpha-low, alpha-high, and beta) is consistent with prior observations (Cantero et al., 1999, 2002; Chen et al., 2008, 2006). Qualitatively, power in the right posterior "hotspot" was somewhat stronger than the left, also replicating prior observations (Lehmann, 1971; Niedermeyer, 2005).

Robustness

Extraction stability

Intentional overextraction did not substantively change the factor structure yielded by the primary SFA. As detailed in Table 1, when we

[3] An exploratory SFA using the covariance matrix, but otherwise similar methods, supported the division of alpha into low (range: 4–8 Hz; peak: 7 Hz) and high (range: 10–12 Hz; peak: 10 Hz) sub-bands with the alpha peak serving as the border.

Table 1
Conventional and SFA-defined EEG frequency bands.

Region (number of channels)	Number of factors	Rotation	Factor rank	Extracted		Rotated		Peak loading (Hz)	Band[a] (Hz)	Prospective label
				Eigenvalue	Variance (%)	Eigenvalue	Variance (%)			
All (129)	Conventional bands	None	–	–	–	–	–	–	08–13	Alpha
			–	–	–	–	–	–	08–10	Alpha-Low
			–	–	–	–	–	–	11–13	Alpha-High
All (129)	5	Varimax	3	3.2	6.4	4.6	9.2	.91 (02)	1–5	Delta
			4	1.5	3.0	3.2	6.3	.86 (08)	6–9	Alpha-Low
			5	1.2	2.4	2.3	4.7	.85 (10)	10–11	Alpha-High
			2	8.5	17.0	7.8	15.6	.88 (14)	12–19	Beta
			1	30.2	60.5	26.8	53.5	.96 (40)	21–49	Gamma
All (129)	6[b]	Varimax	3	3.2	6.4	4.6	9.2	.92 (02)	1–5	Delta
			4	1.5	3.0	3.2	6.5	.87 (08)	6–9	Alpha-Low
			5	1.2	2.4	2.5	5.0	.85 (10)	10–11	Alpha-High
			2	8.5	17.0	7.0	13.9	.88 (14)	12–18	Beta-Low
			1	30.2	60.5	26.6	53.2	.96 (46)	21–49	Gamma
			6	.96	1.9	1.7	3.5	.52 (20)	–	Beta-High
All (129)	4[b]	Varimax	3	3.2	6.4	4.7	9.4	.91 (02)	1–5	Delta
			4	1.5	3.0	3.1	6.1	.84 (08)	6–9	Alpha-Low
			2	8.5	17.0	8.6	17.3	.88 (12)	10–20	Alpha-High
			1	30.2	60.5	27.0	54.0	.96 (46)	21–49	Gamma
Anterior scalp (36)	5	Varimax	3	2.5	5.0	4.5	9.0	.90 (03)	1–5	Delta
			4	1.7	3.4	3.7	7.3	.90 (08)	6–9	Alpha-Low
			5	1.6	3.2	2.3	4.6	.87 (10)	10–11	Alpha–High
			2	6.7	13.4	5.9	11.9	.87 (14)	12–18	Beta
			1	32.1	64.2	28.2	56.4	.96 (47)	18–49	Gamma
Posterior scalp (36)	5	Varimax	3	2.6	5.2	4.5	9.0	.91 (02)	1–5	Delta
			2	10.0	19.9	4.6	9.1	.83 (08)	5–9	Alpha-Low
			4	1.6	3.2	4.4	8.8	.81 (10)	9–11	Alpha-High
			5	1.2	2.4	4.4	8.8	.83 (13)	12–16	Beta
			1	29.7	59.4	27.2	54.4	.98 (40)	21–49	Gamma
Left scalp (36)	5	Varimax	3	3.0	6.0	4.1	8.2	.93 (02)	1–5	Delta
			4	1.5	3.0	3.8	7.6	.84 (07)	6–8	Alpha-Low
			5	1.1	2.2	2.9	5.8	.84 (10)	9–11	Alpha-High
			2	9.3	18.6	6.3	12.7	.89 (14)	12–18	Beta
			1	30.1	60.2	27.8	55.6	.97 (40)	20–49	Gamma
Right scalp (36)	5	Varimax	4	1.5	3.1	4.1	8.3	.91 (02)	1–5	Delta
			3	3.1	6.3	4.7	9.4	.85 (08)	5–9	Alpha-Low
			5	1.3	2.5	3.5	7.0	.79 (10)	10–11	Alpha-High
			2	9.0	18.1	5.5	11.0	.89 (13)	12–17	Beta
			1	29.8	59.7	30.0	54.0	.97 (40)	21–49	Gamma
All (129)	5	Promax[c]	3	3.2	6.4	8.0	[d]	.94 (03)	1–6	Delta
			4	1.5	3.0	7.5	[d]	.93 (08)	5–9	Alpha-Low
			5	1.5	2.4	5.5	[d]	.92 (10)	9–12	Alpha-High
			2	8.5	17.0	16.9	[d]	.94 (16)	12–23	Beta
			1	30.2	60.5	29.4	[d]	.97 (40)	20–49	Gamma

[a] Based on adjacent frequencies with rotated loadings ≥.60.
[b] ± 1 factor from the number determined by Monte Carlo simulations (parallel analysis).
[c] Equivalent results were obtained using an oblimin rotation.
[d] Indeterminate for oblique rotations (e.g., promax).

extracted one factor beyond the number dictated by the Monte Carlo simulation (i.e., parallel analysis), a virtually identical set of bands was identified. Again, alpha split into narrow sub-bands and a distinct theta band was not identified. For its part, the additional factor contained no suprathreshold frequencies. Intentional underextraction did change the factor structure somewhat (Table 1). In particular, the alpha-high and beta bands merged; other bands remained relatively unchanged. The fact that the classical alpha band still fractionated suggests that the division of alpha into sub-bands, with the peak serving as an approximate line of demarcation, is a robust pattern.

Rotational stability

Application of the promax oblique rotation yielded bands that were quite similar to those yielded by varimax (Table 1), suggesting that the data were characterized by relatively well defined latent dimensions (Gorsuch, 1983). Peak loadings and band ranges were generally within 1 Hz of those suggested by varimax rotation. The major difference was the larger number of cross-loadings. For instance, 9 Hz activity loaded on both alpha-low and alpha-high.

Anatomical invariance

The topographic robustness of the solution identified by the primary SFA was examined next. As detailed in Table 1, the overall pattern of the solutions for each of the four ROIs closely resembled that identified by the whole-scalp SFA, suggesting that the solution was reasonably invariant across the scalp. Again, peak loadings and band ranges were generally within 1 Hz of those suggested by the whole-scalp SFA. In particular, the bands associated with the anterior ROI were virtually identical.[4] This suggests that the bands defined by the primary (whole-scalp) SFA were not unduly determined by residual artifact present in channels at the edge of the array, given that they were excluded from the anterior ROI. The other noteworthy observation was that the affiliation of the 9 Hz alpha peak was quite variable. In the case of the anterior and right-hemisphere ROIs, it

[4] Theta is maximal over the frontal midline during demanding cognitive tasks (Mitchell et al., 2008; Sammer et al., 2007). To further assess whether a distinct theta band was identifiable by SFA during quiescence, exploratory SFAs were performed separately for electrode-clusters centered on Fz and FCz. In each case, five or six factors were extracted and varimax or promax rotated. In no case did we identify a factor with suprathreshold loadings in the range of theta but not delta or alpha-low.

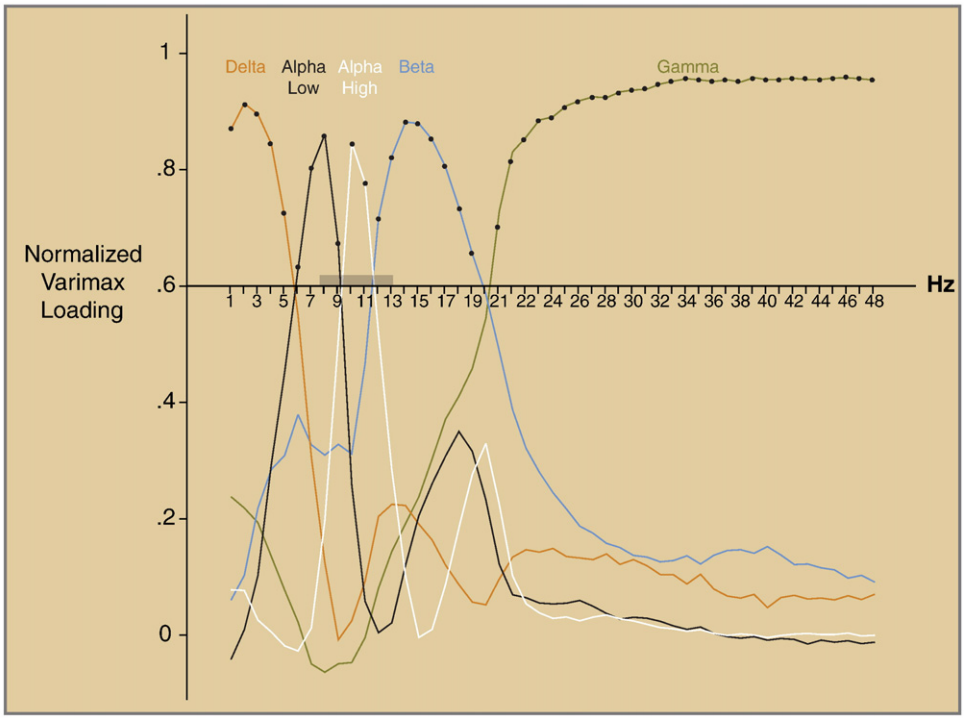

Fig. 2. Varimax-rotated factor loadings for the primary SFA. Horizontal line at .60 indicates the threshold for inclusion in the frequency bands employed in the subsequent tests of sensitivity.

loaded on the alpha-low band; whereas it loaded on both alpha sub-bands in the posterior ROI and the alpha-high sub-band for the left-hemisphere ROI. This instability is consistent the results of the primary SFA (Fig. 2), where 9 Hz showed quantitatively similar loadings on both alpha sub-bands.

Sensitivity

Individual differences in tonic activity

We next examined whether the various alpha bands differed in their sensitivity to variation in the BIS. Because in-depth analyses for the conventional (i.e., *a priori*) alpha-low band (8–10 Hz) have been presented elsewhere (Shackman et al., 2009a), results are only briefly summarized here.

On the scalp, individuals who showed greater right-midfrontal activity rated themselves higher on the BIS. Relations between the BIS and midfrontal asymmetry were virtually identical across alpha bands ($rs(48) = -.47$ to $-.50$, corrected $ps < .008$) and differences among them were not significant, $ps > .47$.[5] This was consistent with the strong correlations among midfrontal asymmetry scores derived using the various alpha bands, $rs = .99$ to $.88$, $ps < .001$. Analyses performed in the intracerebral source-space using the LORETA algorithm yielded the same conclusion (see the Supplement).

[5] Exploratory analyses were also performed on the scalp using bands derived from participants' peak individual alpha frequency (IAF). For the primary sample, most participants showed peak power at 9 Hz (43%). The distribution was approximately normal, with smaller percentages at 10 Hz (33%), 8 Hz (16%), 7 Hz (4%) and 11 Hz (4%). By convention (Klimesch, 1999), IAF was then used to create individually tailored microbands: alpha-1 (IAF −4 Hz to IAF −2 Hz), alpha-2 (IAF −2 Hz to IAF), and alpha-3 (IAF to IAF +2 Hz). Data reduction and analyses were otherwise identical to those used for our key hypothesis tests. Results indicated that relations between mid-frontal asymmetry and BIS were similar in magnitude to the conventional and SFA-defined alpha bands. For IAF, relations were strongest for the alpha-1 microband ($r = -.51$), which did not differ from alpha-2 ($r = -.43$) and alpha-3 ($r = -.44$), $ps > .11$.

Mean differences in task-induced activation

In the secondary sample, power in the alpha range peaked at ~10.5 Hz in both the eyes-open ($M = 10.5$ Hz, $SD = 1.2$) and eyes-closed conditions ($M = 10.5$ Hz, $SD = 1.4$), $p = .77$. Topographic plots of mean spectral power density, collapsed across conditions, for each of the bands identified by SFA in the primary sample are depicted in Fig. 4. The topographies are similar to those for the primary sample (Fig. 3). Again, prominent activity in the low-frequency delta and high-frequency gamma bands was observed at electrodes along the edge of the array (Fig. 4), particularly among anterior channels neighboring the face and eyes. This suggests that residual ocular and myogenic activity was present following ICA-based artifact attenuation. Despite differences in size and peak alpha frequency, the factor structure for the secondary sample closely resembled that of the primary sample (Supplementary Table 4).

Fig. 5 presents the eyes-open vs. eyes-closed contrast for both conventional and SFA-defined bands. Visual inspection indicated that the modulation of alpha power in response to eye-opening was more mesial than the region of greatest power density (Fig. 4). We first examined the degree to which SFA-defined alpha bands were sensitive to the eye-opening manipulation, a traditional hallmark of alpha activity. General linear models (GLM) with Huynh-Feldt corrections, performed separately for each of the representative channels presented in Table 2, indicated that the impact of the eye-opening manipulation differed across the five SFA-defined bands, $Fs(4, 64) > 15.9$, $ps < .001$. Follow-up analyses revealed that the SFA-defined alpha-high band (10–11 Hz) displayed a greater reduction in power than the other bands, $ps < .02$. Consistent with prior work (Chen et al., 2008; Davidson et al., 1990; Kuhlo, 1976; Motokizawa and Fujimori, 1964; Volavka et al., 1967), smaller, but still significant reductions were observed throughout the spectrum, particularly at midline parieto-occipital channels (Fig. 5 and Table 2). Outside of this region, effects in the delta and gamma bands were not significant.

Planned contrasts were then used to test whether the various alpha bands differed from one another at representative channels. Consistent with Fig. 5, this revealed that the use of narrow alpha sub-

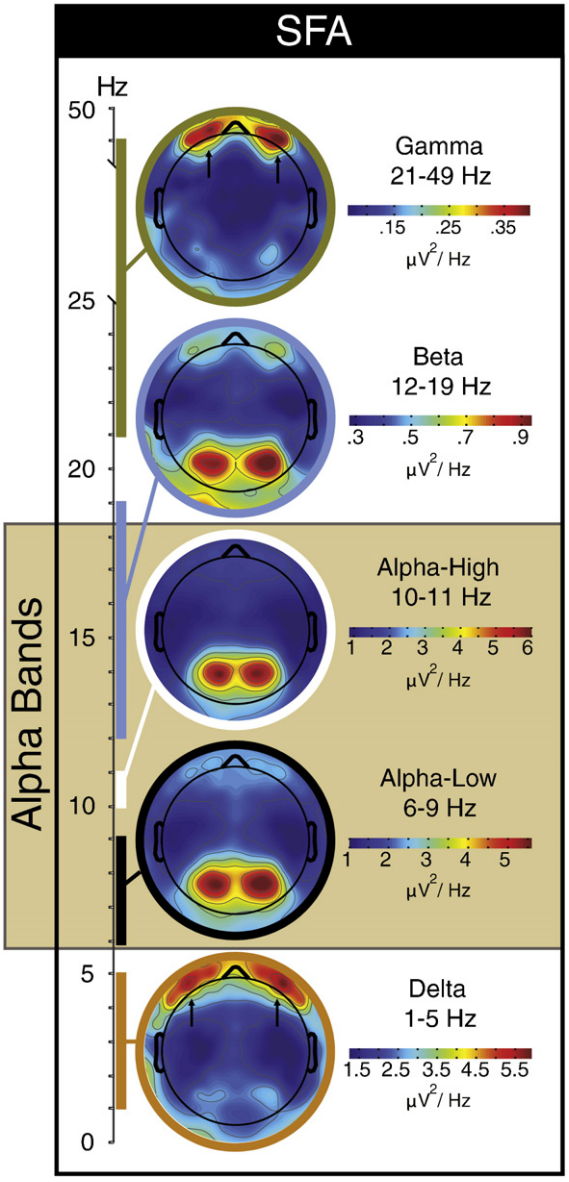

Fig. 3. Spline-interpolated mean power in the primary sample for each SFA-defined band. Bands were derived by thresholding (≥.60) varimax-rotated loadings and weighting each suprathreshold frequency equally. Colors indicate spectral power (μV^2/Hz). To maximize bandwidth, the color overlays were separately adjusted to the range defined by each factor. Consequently, *like colors are not comparable across plots*. Vertical axis shows the range of frequencies spanned by each band. Note the apparent presence of residual artifact in the delta and gamma bands at anterior sites following standard artifact *rejection* procedures (arrows).

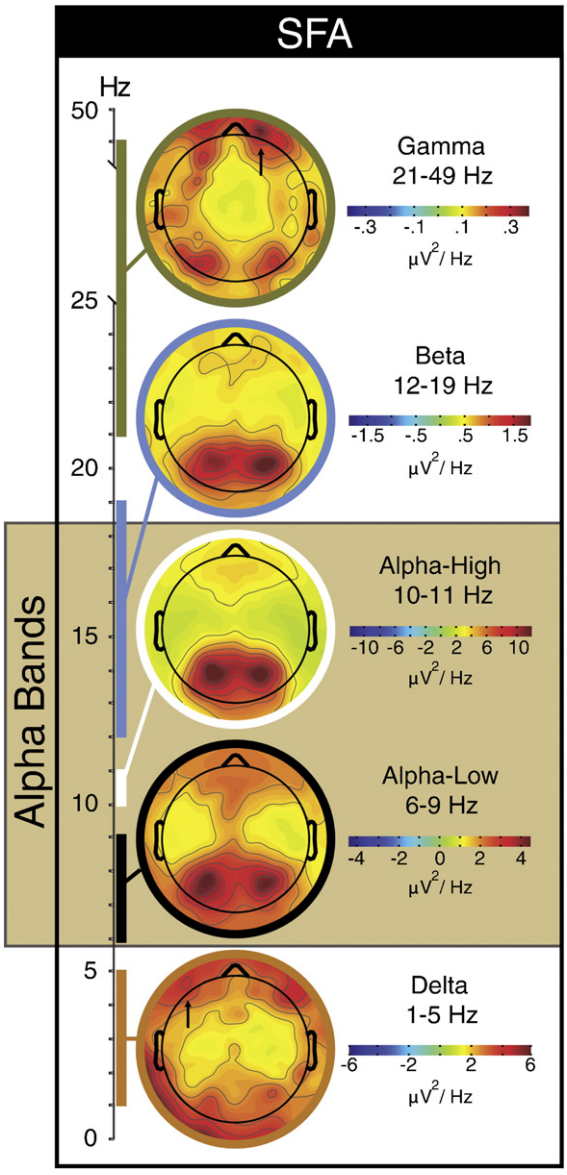

Fig. 4. Spline-interpolated mean power in the secondary sample ($n = 17$) for each SFA-defined band. Bands were defined by SFA performed on the *primary* sample. Figure conventions are the same as Fig. 3.

bands failed to increase sensitivity over that achieved by the classic alpha band. In the case of conventional bands, there was no difference between alpha-wide (8–13 Hz) and alpha-low (8–10 Hz), $ps > .42$. Indeed, the conventional alpha-high sub-band (11–13 Hz) proved somewhat less sensitive than the broadband for the grand average ($p = .05$) and Fz ($p = .06$) channels; the conventional high and low sub-bands did not differ from one another, $ps > .17$. In the case of SFA-defined bands, it was the low sub-band (6–9 Hz) that showed reduced sensitivity compared to alpha-wide ($ps < .01$), whereas the alpha-high band (10–11 Hz) did not differ ($ps > .32$). In the SFA case, alpha-high was more sensitive than alpha-low, $ps < .02$.

Inspection of the spectra depicted in Fig. 5 suggests that all of these differences in sensitivity represent predictable consequences of the degree to which the bands incorporated the frequencies showing the largest difference across conditions. For instance, the reduced sensitivity of SFA-defined alpha-low is likely a consequence of diluting the large difference at 8–9 Hz with the much smaller difference at 6–7 Hz. Consistent with this perspective, exploratory analyses demonstrated that simply centering a window at the peak (9–11 Hz), performed about as well as the conventional wideband at representative channels, $ts(16) = 6.4–7.6$, $ps < .001$.[6]

[6] Exploratory logistic regression analyses, in which the individual *frequencies* were used to classify condition (eyes-closed vs. eyes-open), yielded the same conclusion (Fabiani et al., 1987; Poolman et al., 2008). Using stepwise models with backwards elimination, the only significant predictor of condition was 10 Hz activity, where the difference in activity across conditions was maximal (Fig. 5). This pattern was observed across both anterior and posterior electrodes. This implies that neighboring frequencies in the classical alpha range provided largely redundant sources of information about between-condition variance. Using a similar strategy but with forced entry of *bands*, we also observed that the classification performance of the classical alpha band was similar to that of each combination of sub-bands (conventional or SFA-defined), indicating that the greater parsimony of the classical band did not come at the expense of sensitivity.

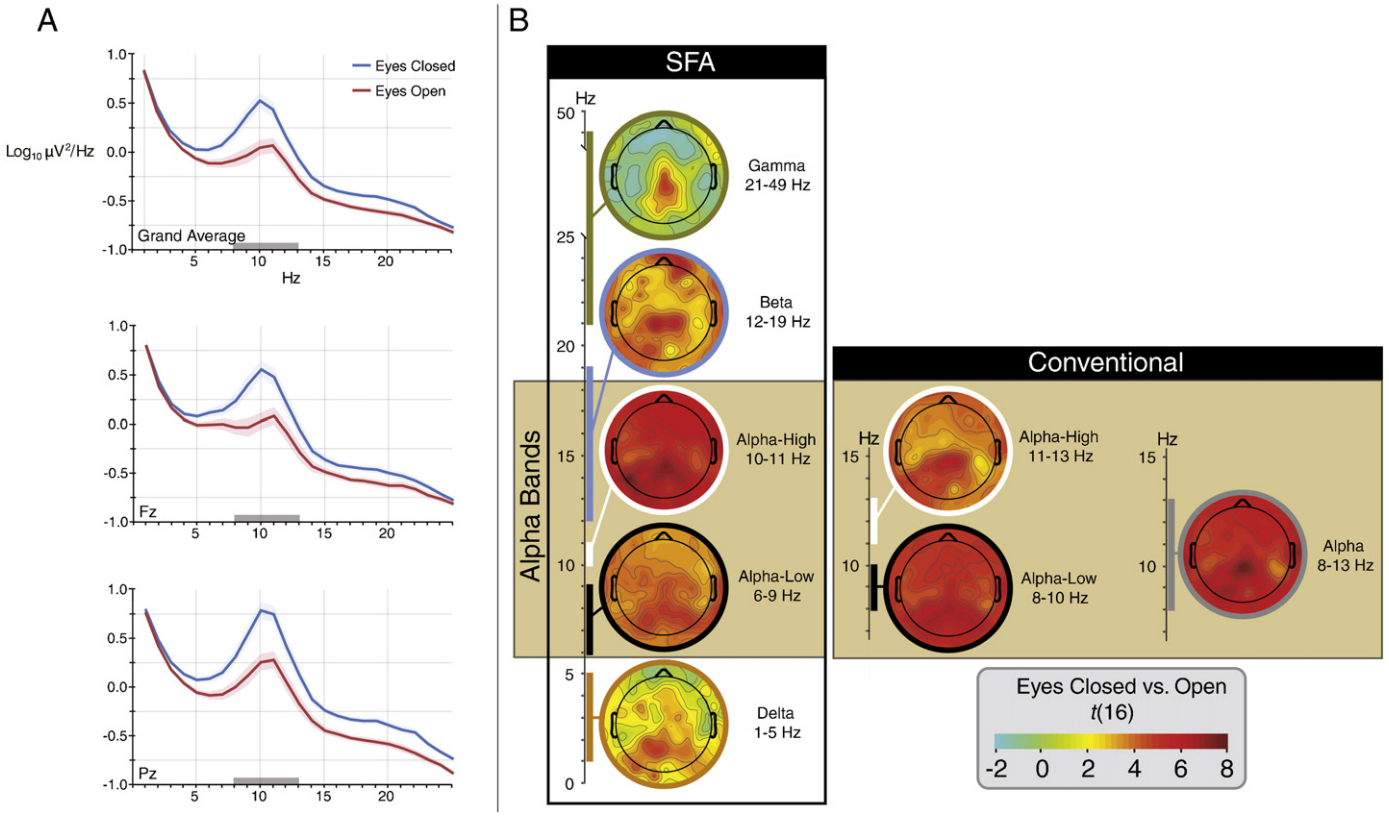

Fig. 5. Sensitivity to induced activation in the secondary sample. Both panels depict the eyes-closed vs. eyes-open contrast. (A) Power spectra for each condition. Statistical confidence envelopes indicate the nominal probability of the null hypothesis being rejected by chance: $p<.05$ (non-overlapping envelopes) or $p>.05$ (overlapping envelopes). Envelopes were computed for each frequency by taking one-quarter of the range spanned by the 95% CI of the mean difference, equivalent to $(M/N)^{1/2}\times S/2$ (where M is the mean square error, N is the number of cases, and S is the Studentized range statistic) (http://www.lrdc.pitt.edu/schunn/SSB/index.html). Gray bar along the x-axis indicates the classical alpha band. (B) Spline-interpolated topographic maps of the t-test for each band computed separately at each electrode ($t=2.12$, uncorrected $p=.05$). SFA and conventionally defined bands are depicted on the left and right sides of the panel, respectively. Additional figure conventions are the same as Fig. 3.

Post hoc analyses of ICA-based artifact correction

In contrast to several of our recent reports (McMenamin et al., 2010, 2009), the aim of the present study was not to assess methods for EEG artifact reduction. Indeed, we did not anticipate prominent artifacts, given that participants were resting quietly for relatively short periods. Contrary to expectation, we observed apparent residual artifact in the delta and gamma bands at electrodes neighboring the face and eyes. This was especially prominent in the primary sample (Fig. 3), where a threshold-based procedure was used to reject artifact-contaminated epochs, but was also apparent in the secondary sample (Fig. 4), where ICA was used to attenuate artifacts.

In order to determine whether it was possible to further minimize such artifacts, we qualitatively assessed the impact of using a more stringent ICA-based protocol (for details, see McMenamin et al., 2010). As before, components containing gross, ocular, or clear-cut muscle artifacts were rejected. In addition, components that were unclassifiable (i.e., noise), accounted for trivial amounts of variance (<0.2%), or contained any signs of muscle artifact whatsoever were discarded.

Fig. 6 depicts topographic plots of mean power density for each the five SFA-defined bands following this "maximal" ICA-based artifact correction. Visual inspection suggests that the artifacts contaminating anterior electrodes were largely eliminated. Exploratory analyses of the eyes-open vs. eyes-closed contrast revealed a pattern similar to that reported above for the secondary sample (not reported), providing some evidence of specificity. In general, maximal ICA-based correction was associated with small increases in sensitivity among the alpha bands, consistent with prior work (Zeman et al., 2007). As one might expect, this increase was more pronounced for the delta and gamma bands. For instance, power suppression in response to eye opening was reliable in the gamma band at all of the representative channels following maximal ICA-based correction, $ps<.001$.

Discussion

The present study sought to answer two fundamental questions about the frequency bands yielded by SFA. First, are they robust? Second, in the case of alpha-like activity, do they increase sensitivity? Using a rigorous combination of psychometric and electrophysiological techniques, we identified five bands in the high-density tonic EEG (Fig. 2): delta (1–5 Hz), alpha-low (6–9 Hz), alpha-high (10–11 Hz), beta (12–19 Hz), and gamma (21–49 Hz). Although the peak loadings and boundaries varied by ~1 Hz, this basic pattern proved quite robust across variations in SFA methodology and regions of the scalp (Table 1). It was also identified in the smaller secondary sample (Supplementary Table 4).[7]

The present study also provides novel evidence that narrow alpha sub-bands are no more sensitive than the classical broadband to individual differences in tonic activity or mean differences in task-induced activity. This was true for sub-bands that were pre-defined according to convention or empirically defined using SFA. In

[7] The exact boundaries of these bands are expected to vary somewhat across studies as a function of data reduction parameters (Harris, 1978b; Lopes da Silva, 2005) and demographic variables, such as age (Aurlien et al., 2004; Dustman et al., 1999; van Albada et al., 2010).

Table 2
Eyes-closed vs. eyes-open.[a]

Band (Hz)	Channel (s)	Closed	Open	Difference	
		M (SD)	M (SD)	*t*	*p*
SFA Delta (1–5)	Range	–	–	−1.4 to 5.8	<.98
	Average	3.5 (1.0)	3.4 (1.1)	−1.7	.11
	Fz	3.0 (1.8)	2.6 (1.4)	−1.3	.22
	Pz	3.5 (1.7)	2.8 (1.4)	−4.7	<.001
Alpha (8–13)	Range	–	–	−4.4 to 8.4	<.001
	Average	3.9 (2.4)	1.5 (1.5)	−6.4	<.001
	Fz	3.9 (3.6)	1.5 (2.0)	−6.1	<.001
	Pz	9.3 (8.0)	2.9 (4.4)	−7.6	<.001
Alpha-Low (8–10)	Range	–	–	−4.6 to 7.1	<.001
	Average	4.8 (4.3)	1.5 (1.5)	−6.2	<.001
	Fz	5.2 (6.4)	1.6 (2.2)	−6.1	<.001
	Pz	9.5 (9.9)	2.7 (3.5)	−7.1	<.001
SFA Alpha-Low (6–9)	Range	–	–	−3.4 to 5.8	<.004
	Average	2.9 (3.1)	1.1 (0.8)	−4.8	<.001
	Fz	3.4 (4.9)	1.4 (1.5)	−4.1	.001
	Pz	4.5 (5.8)	1.6 (1.6)	−5.8	.001
Alpha-High (11–13)	Range	–	–	−2.9 to 7.0	<.02
	Average	3.0 (2.2)	1.4 (1.6)	−4.6	<.001
	Fz	2.7 (2.1)	1.4 (1.9)	−4.0	.001
	Pz	9.0 (9.8)	3.1 (5.5)	−5.8	.001
SFA Alpha-High (10–11)	Range	–	–	−4.4 to 8.0	<.001
	Average	5.6 (4.1)	2.2 (3.3)	−6.4	<.001
	Fz	5.3 (4.8)	2.2 (3.9)	−6.4	<.001
	Pz	15.2 (16.8)	5.0 (10.2)	−7.3	<.001
SFA Beta (12–19)	Range	–	–	−2.2 to 9.5	<.05
	Average	0.9 (0.6)	0.5 (0.2)	−4.5	<.001
	Fz	0.8 (0.5)	0.5 (0.3)	−3.5	.003
	Pz	2.1 (2.8)	0.8 (0.6)	−5.8	<.001
SFA Gamma (21–49)	Range	–	–	−2.1 to 5.2	<.98
	Average	0.1 (0.0)	0.1 (0.1)	−0.4	.73
	Fz	0.1 (0.0)	0.1 (0.0)	−0.4	.70
	Pz	0.1 (0.1)	0.1 (0.0)	−4.6	<.001

[a] Descriptive statistics are in units of μV^2/Hz (i.e., *not* $\log_{10}$-transformed) to permit direct comparison with other analyses. By convention, *t*-tests were computed using $\log_{10}$-transformed μV^2/Hz.

particular, frontal asymmetry (i.e., laterality) metrics derived from each of the alpha bands proved comparably sensitive to individual differences in the BIS ($rs = -.47$ to $-.50$). The same conclusion was reached for LORETA analyses in the intracerebral source-space (see the Supplement). These null results are consistent with the visually similar topographies of the SFA-defined alpha sub-bands (Figs. 3 and 4) and the high degree of redundancy across frontal asymmetry scores derived from each of the alpha bands (77–98% shared variance; Supplementary Table 3).

The sensitivity of the alpha bands to mean differences in task-induced oscillatory activity was also assessed. Visual stimulation (i.e., eyes-open vs. -closed) suppressed power across the spectrum, with peak differences in the alpha range (Fig. 5 and Table 2). The size of this effect was *never* larger for the narrow sub-bands. In fact, the classical broadband definition of alpha exhibited greater sensitivity than several of them. Follow-up analyses suggested that differences in sensitivity were largely a function of the degree to which each of the alpha bands was centered on the frequencies showing peak differences across conditions.

Alpha at rest and in action

The present study indicates that the dissociation of alpha-range frequencies into upper and lower sub-bands is a robust phenomenon. The biophysical source of this split is unclear, although it may represent a consequence of bimodal alpha peaks. Chiang et al. (2008) recently reported that 48 of 100 participants exhibit two alpha peaks. Interestingly, these occurred at ~8 and ~10 Hz, similar to the peak loadings we obtained for the upper and lower alpha bands in the primary SFA (Table 1).

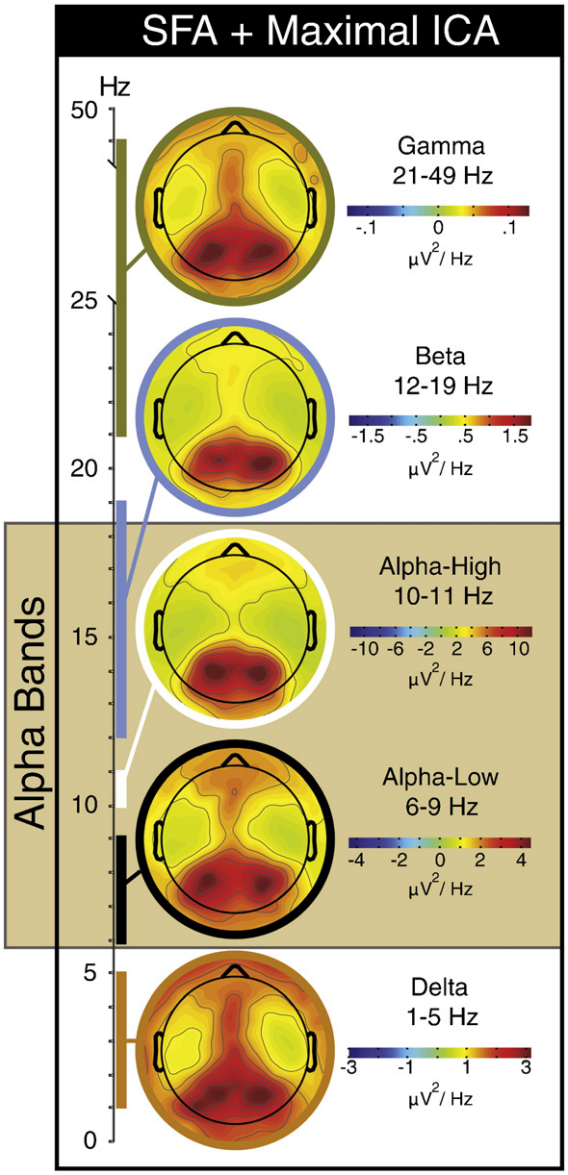

Fig. 6. Spline-interpolated mean power in the secondary sample for each SFA-defined band following stringent ("maximal") ICA-based artifact correction. Figure conventions are the same as Fig. 3.

Regardless of the underlying source of the alpha sub-bands, we uncovered no evidence that honoring this distinction increases sensitivity to individual differences in tonic activity or mean differences in task-induced activation. In the case of tonic activity, the present results are consistent with the existing literature (reviewed in the Introduction); inconsistencies and null results are what one would expect to obtain across samples and individual differences measures if upper and lower alpha do not substantially differ in their sensitivity.

Given both the strengths and limitations of the present study, we refrain from recommending that EEG researchers eschew the narrow alpha bands. Further research is required to more fully address this question. In particular, it would be profitable to assess the degree to which these results generalize to other measures of emotion and motivation (for further discussion, see Shackman et al., 2009a). Nevertheless, there are reasons aside from parsimony for using the classical broadband definition (8–13 or 8–12 Hz). In particular, the broadband seems better able to accommodate variation in peak alpha frequency. As noted earlier, peak alpha frequency varies across

individuals ($SD = \sim 1$ Hz; Footnote 5). Furthermore, analyses of the running mean (Goncharova and Barlow, 1990) and amplitude modulation (i.e., "waxing-and-waning;" Barlow, 1993; Schroeder and Barr, 2000) suggest that the peak frequency can vary by ~2 Hz over successive measurements.

Investigators interested in using narrow bands should consider techniques for optimizing data collection and preprocessing. These include the use of longer FFT epochs, which increases the nominal frequency resolution and minimizes spectral artifacts that can potentially inflate dependencies across adjacent bands (Harris, 1978a). It may also be helpful to center bands on each individual's peak alpha frequency (Klimesch, 1999), particularly in small samples (Footnote 5). In general, if narrow bands are employed for tonic EEG research, the classical broadband should also be assessed. Finally, claims about differential sensitivity across sub-bands must be supported by the appropriate statistical comparisons.

The present results suggest that the use of narrow alpha sub-bands, whether defined *a priori* or using SFA, can reduce sensitivity to mean differences in task-induced oscillatory activity. The simplest and most convenient alternative is to employ the conventional broadband, although this carries with it the risk of mixing heterogeneous effects (Klimesch, 1999). A better alternative, common in event-related potential (ERP) and event-related spectral perturbation (ERSP) studies, is to define a band based on visual or algorithmic interrogation of the spectrum (Fabiani et al., 1987; Kramer, 1985). An increasingly tractable approach is to compute tests at every frequency and electrode, appropriately corrected for temporal autocorrelation and multiple comparisons. Common correction procedures make use of permutation or randomization (Anderson and ter Braak, 2003; Maris and Oostenveld, 2007; Nichols and Holmes, 2007; Wyart and Tallon-Baudry, 2008) or the False Discovery Rate (FDR; Busch et al., 2009; Edwards et al., 2009; Nichols, 2007) and are implemented in several software packages.[8] It may be useful to employ a hierarchical analytic approach in which bands are initially identified using a summary measure, such as the average spectrum across a region-of-interest or the standard deviation of spectra across electrodes (i.e., analogous to global field power in the time-domain; Michel et al., 1995; Murray et al., 2008), and then inferential tests are performed at each electrode using the usual measure of log-transformed power density. This strategy has the advantage of minimizing the number of comparisons, potentially increasing statistical power. In some cases, down-sampling the spectrum or time-frequency space affords similar advantages (Edwards et al., 2009).

Alpha's neighbors: theta and beta

Consistent with the absence of a theta peak in the raw spectrum (Fig. 1), SFA failed to identify a distinct theta band during quiescence in either sample (Table 1 and Supplementary Table 4). Frequencies in the classical theta range (4–8 Hz) were instead apportioned to the neighboring delta and alpha-low bands (Fig. 2). This was true even for analyses that were restricted to the frontal midline regions that have been most consistently associated with task-induced theta activation (Footnote 4).

Could it be that the band we have labeled 'alpha-low' (range: 6–9 Hz; peak factor loading: 8 Hz) is, in fact, theta? This is highly unlikely—indeed, the present results provide compelling evidence that the SFA-defined 6–9 Hz band satisfies the spectral, topographic, and functional criteria that conventionally define alpha (reviewed in the Introduction). First, comparison of the raw spectrum (Fig. 1) to the SFA loadings (Fig. 2) indicates that the 6–9 Hz range contains most of the spectral activity typically associated with alpha, including the peak at 9 Hz. Second, the topography of activity in the 6–9 Hz range was virtually identical to that characterizing the adjacent alpha-high sub-band (range: 10–11 Hz; peak: 10 Hz). Both exhibited maximal power at bilateral parieto-occipital electrodes (Figs. 3 and 4). Finally, activity in the 6–9 Hz band was reliably suppressed, particularly at midline parieto-occipital electrodes, in response to visual stimulation (Fig. 5 and Table 2).

Whereas this conclusion is contrary to classical EEG taxonomies (Brazier et al., 1961; Niedermeyer, 2005; Nuwer et al., 1999), it is in line with research indicating that the theta rhythm is uncommon during quiet wakefulness in healthy adults. For instance, several very large studies have demonstrated that <1% of patients referred to clinical EEG departments over a multi-year period (Okada and Urakami, 1993; Palmer et al., 1976; Westmoreland and Klass, 1986) and only ~8% of unselected military personnel exhibit frank midline theta rhythms at rest (Takahashi et al., 1997), although higher proportions have occasionally been reported (Bocker et al., 2009). On the basis of this kind of evidence, it has been argued that theta is relatively rare in the tonic EEG of fully awake adults (Schacter, 1977; Westmoreland and Klass, 1990).

Task-induced activation in the theta band also seems to be a less robust phenomenon. During demanding cognitive tasks, it has been reported that scalp-recorded oscillatory activity in the theta range increases over the frontal midline (e.g., Mitchell et al., 2008; Sammer et al., 2007). Intracerebral recordings in humans and nonhuman primates have shown a broadly similar pattern, with theta activity often identified with the anterior cingulate (Lakatos et al., 2008; Raghavachari et al., 2001; Steinvorth et al., 2010; Tsujimoto et al., 2010; Wang et al., 2005; Womelsdorf et al., 2010). Nevertheless, a number of investigators have suggested that task-induced theta activity is not exhibited in a sizable number of participants (Inanaga, 1998; Meltzer et al., 2007; Niedermeyer, 2005) or is not present on a large proportion of trials (Onton et al., 2005). Such observations suggest that it may be necessary to use alternatives to SFA for decomposing the spectrum, such as ICA, in order to obtain reliable indices of scalp-recorded theta activity (Onton et al., 2005). In cases where task-induced theta oscillations are plausible, it might also prove fruitful to employ covariance-based SFA.

In contrast to theta, the beta band was consistently identified by SFA in both samples. The present study provides new evidence that beta, or as it is sometimes termed, the "lower" beta band (~13–20 Hz), is closely related to alpha. The two bands strongly resembled one another both topographically (Figs. 3 and 4) and functionally (Table 2). Furthermore, when we performed SFA with intentional underextraction, the alpha-high and beta bands fused (Table 1), underscoring their shared variance. Our conclusion that the two bands are closely related is consistent with both recent speculations (Chen et al., 2008; van Albada et al., 2010) and an older literature suggesting that the posterior beta rhythm is simply a fast variant of alpha (Kuhlo, 1976).

Artifact at the edges: delta and gamma

Quite unexpectedly, prominent artifact was observed at the anterior edge of the electrode array in the SFA-defined delta and gamma bands (Figs. 1, 3, and 4). Notably, this was found using ostensibly 'artifact-free' data. That the delta and gamma bands are vulnerable to ocular, muscular, and movement artifacts is well established and uncontroversial. In particular, numerous investigations over the past half century have suggested that much of the variance in waking delta activity is attributable to ocular sources (Chen et al., 2008; Gasser et al., 1992; Gibbs, 1942; Herrmann et al., 2001; Sakamoto et al., 2010). This view is consistent with demonstrations that tonic power in the delta band is less heritable and less reliable than the other classical bands (Smit et al., 2005; Tomarken et al., 1992b; Van Albada et al., 2007). Similar evidence suggests that

[8] Including EEGLAB (http://sccn.ucsd.edu/eeglab), EMSE (http://www.source-signal.com), and Fieldtrip (http://fieldtrip.fcdonders.nl).

scalp-recorded gamma activity is often myogenic (McMenamin et al., 2010; Shackman et al., 2009b; Whitham et al., 2008).

The key contribution of the present report was to demonstrate that the application of conventional threshold-based rejection or ICA-based correction procedures is not sufficient to completely attenuate such artifacts. Interestingly, the use of a more stringent (i.e., "maximal") ICA-based protocol did appear to eliminate them (Fig. 6). But whether that procedure exhibits adequate specificity (i.e., preserves neurogenic activity) in the highest and lowest frequency bands is unclear and cannot be resolved by the present study. This represents a challenging but useful avenue for future methodological research (see also McMenamin et al., 2010).

It is plausible that such artifacts influenced the results of the SFAs reported here. Indeed, exploratory SFAs of the dataset subjected to the maximal ICA procedure yielded bands that differed from those identified by the other factor analyses. In particular, the delta and lower alpha bands were fused (Supplementary Table 4). This provides evidence, albeit circumstantial, that the primary difference between delta and alpha is the degree of residual artifact. Nevertheless, it is not clear that this fusion simply reflects the elimination of residual artifact. For instance, SFA of the primary dataset indicated dissociation of the two bands in the posterior region of the array, far removed from the assumed source of the artifact (Table 1). Thus, it might be some unintended consequence of the maximal ICA procedure that led delta and alpha-low to merge (i.e., low specificity for separating neurogenic from artifactual delta sources).

In light of these findings, we strongly recommend that investigators with a substantive interest in the delta (e.g., Knyazev, 2007; Knyazev et al., 2009; Wacker et al., 2009) or gamma bands (e.g., Yuval-Greenberg et al., 2008) routinely publish scalp topographies. Preferably, topographic maps would be split by group or condition and include the most anterior electrodes recorded. Unfortunately, it has become increasingly common for studies reporting effects in these bands to omit such maps, making it difficult for others to independently judge whether key effects are indeed neurogenic (Shackman, 2010). This omission seems to be particularly frequent in source modeling ("localization") investigations. In cases where it is plausible that effects are artifactual, special controls (Darvas et al., 2010; Henriques and Davidson, 1991; Karson et al., 1987; Keren et al., 2010; Rihs et al., 2009; Shackman et al., 2009a) or more complex artifact correction procedures should be employed (Keren et al., 2010; Kierkels et al., 2007; McMenamin et al., 2010). The present results suggest that the intelligent application of artifact correction procedures, such as ICA, has the potential to enhance sensitivity to genuine neurogenic effects in the delta and gamma bands.

Decomposing the EEG: SFA and beyond

The use of SFA to derive EEG frequency bands is founded on two ideas. First, from a methodological perspective, it is assumed that rotated eigenvectors are a reasonable set of bases for decomposing the EEG. Put differently, that the neural sources of the different frequencies are mixed according to the assumptions of the factor analytic model. But whether this assumption is reasonable is difficult to know. Certainly there are alternative techniques, founded on somewhat different assumptions, for separating spectral sources (Anemuller et al., 2003; Hyvarinen et al., 2010; Makeig et al., 2004, 2002). Identifying the statistical model that best fits the EEG will require a deeper understanding of the biophysical bases of scalp-recorded oscillations (Buzsaki, 2006; Nunez and Srinivasan, 2005). Investigations that employ intracranial EEG recordings (Edwards et al., 2009; Manning et al., 2009; Palva and Palva, 2007; Whittingstall and Logothetis, 2009) or simultaneous electrophysiological and hemodynamic measurements (He et al., 2008; Mantini et al., 2007; Ojemann et al., 2010; Rosa et al., 2010) may help to resolve this uncertainty.

The second idea underlying the use of SFA in EEG research is that by optimally organizing the multidimensional spectral data into unidimensional bands, it can improve sensitivity. The problem is that SFA is not especially well suited to this aim, as some researchers noted many years ago (Donchin and Heffley, 1978). SFA acts blindly, without any knowledge about the subset of variance—that is, the individual or mean differences variance—that is of interest. This stands in contrast to more recently developed techniques that restrict the decomposition to the subset that is most informative about the activity of interest. Such techniques include constrained PCA (cPCA; Woodward et al., 2006), partial least squares (PLS; McIntosh and Lobaugh, 2004), and principal components regression (PCR; Varmuza and Filzmoser, 2009).[9] Such multivariate techniques represent a useful and potentially more sensitive alternative to SFA or to the massively univariate testing procedures described earlier.

Conclusions

> *In the course of generating behavior, the brain also generates time-varying electric and magnetic fields. The aim of electroencephalography is to record and measure samples of these fields during certain states and sequences of behavior, in order to explain some of the mechanisms by which behavior is generated.* (Freeman, 1987, p. 583)

In the frequency-domain, the choice of bands entails a decision about the physical, statistical, and psychological filters one wishes to impose upon the power spectrum. As such, it fundamentally constrains the inferences and explanations that that can be validly extracted from the EEG. This is especially true when insufficient attention is paid to the topographies associated with the different frequency bands and to the raw spectra that underlie banded power densities. Increased diligence to these routine procedures, particularly when combined with recently developed analytic tools for interrogating the EEG, will have substantial benefits for understanding the contributions of neural oscillations to adaptive and maladaptive behavior.

Acknowledgments

The first two authors contributed equally to this study. We thank Donna Cole, Isa Dolski, Andrew Fox, Aaron Heller, Laura Friedman, Donald McLaren, Bradley Postle, Jessica Shackman, Jonathan Shackman, Aaron Teche, Barry Van Veen, and three anonymous reviewers for assistance and NIMH (P50-MH52354 and MH43454 to RJD) for support. BM was supported by NIH T32-HD007151. Authors acknowledge no conflicts of interest.

Appendix A. Supplementary data

Supplementary data associated with this article can be found, in the online version, at doi:10.1016/j.neuroimage.2010.03.037.

References

Anderson, M.J., ter Braak, C.J.F., 2003. Permutation tests for multi-factorial analysis of variance. J. Stat. Comput. Simul. 73, 85–113.

Andresen, B., 1993. Multivariate statistical methods and their capability to demarcate psychophysiologically and neurophysiologically sound frequency components of human scalp EEG. In: Zschocke, S., Speckmann, E.-J. (Eds.), Basic Mechanisms of the EEG. Birkhauser, Boston, pp. 317–352.

Anemuller, J., Sejnowski, T.J., Makeig, S., 2003. Complex independent component analysis of frequency-domain electroencephalographic data. Neural Netw. 16, 1311–1323.

Arruda, J.E., Weiler, M.D., Valentino, D., Willis, W.G., Rossi, J.S., Stern, R.A., et al., 1996. A guide for applying principal-components analysis and confirmatory factor analysis to quantitative electroencephalogram data. Int. J. Psychophysiol. 23, 63–81.

[9] Software implementing cPCA (http://www3.telus.net/Todd_S_Woodward/cpca_links.htm) and PLS (http://www.rotmanbaycrest.on.ca/pls) for neurophysiological analyses is freely available.

Aurlien, H., Gjerde, I.O., Aarseth, J.H., Eldoen, G., Karlsen, B., Skeidsvoll, H., et al., 2004. EEG background activity described by a large computerized database. Clin. Neurophysiol. 115, 665–673.

Babiloni, C., Sara, M., Vecchio, F., Pistoia, F., Sebastiano, F., Onorati, P., et al., 2009. Cortical sources of resting-state alpha rhythms are abnormal in persistent vegetative state patients. Clin. Neurophysiol. 120, 719–729.

Barlow, J.S., 1993. The Electroencephalogram. Its Patterns and Origins. MIT Press, Cambridge, MA.

Bell, A.J., Sejnowski, T.J., 1995. An information-maximization approach to blind separation and blind deconvolution. Neural Comput. 7, 1129–1159.

Berger, H., 1929/1969. On the Electroencephalogram of Man. The Fourteen Original Reports on the Human Electroencephalogram (P. Gloor, Trans.). Elsevier, NY.

Blackhart, G.C., Minnix, J.A., Kline, J.P., 2006. Can EEG asymmetry patterns predict future development of anxiety and depression? A preliminary study. Biol. Psychol. 72, 46–50.

Bocker, K.B., Hunault, C.C., Gerritsen, J., Kruidenier, M., Mensinga, T.T., Kenemans, J.L., 2009. Cannabinoid modulations of resting state EEG theta power and working memory are correlated in humans. J. Cogn. Neurosci. (Electronic publication before publication). doi:10.1162/jocn.2009.21355.

Boutros, N.N., Arfken, C., Galderisi, S., Warrick, J., Pratt, G., Iacono, W., 2008. The status of spectral EEG abnormality as a diagnostic test for schizophrenia. Schizophr. Res. 99, 225–237.

Brazier, M.A.B., Cobb, W.A., Fischgold, H., Gastault, H., Gloor, P., Hess, R., et al., 1961. Preliminary proposal for an EEG terminology by the terminology committee for the International Federation for Electroencephalography and Clinical Neurophysiology. Electroencephalogr. Clin. Neurophysiol. 13, 646–650.

Busch, N.A., Dubois, J., VanRullen, R., 2009. The phase of ongoing EEG oscillations predicts visual perception. J. Neurosci. 29, 7869–7876.

Buss, K.A., Schumacher, J.R.M., Dolski, I., Kalin, N.H., Goldsmith, H.H., Davidson, R.J., 2003. Right frontal brain activity, cortisol, and withdrawal behavior in 6-month-old infants. Behav. Neurosci. 117, 11–20.

Buzsaki, G., 2006. Rhythms of the Brain. Oxford University Press, NY.

Cantero, J.L., Atienza, M., Gomez, C., Salas, R.M., 1999. Spectral structure and brain mapping of human alpha activities in different arousal states. Neuropsychobiology 39, 110–116.

Cantero, J.L., Atienza, M., Salas, R.M., 2002. Human alpha oscillations in wakefulness, drowsiness period, and REM sleep: different electroencephalographic phenomena within the alpha band. Neurophysiol. Clin. 32, 54–71.

Carver, C.S., Harmon-Jones, E., 2009. Anger is an approach-related affect: evidence and implications. Psychol. Bull. 135, 183–204.

Carver, C.S., White, T.L., 1994. Behavioral inhibition, behavioral activation, and affective responses to impending reward and punishment: the BIS/BAS Scales. J. Pers. Soc. Psychol. 67, 319–333.

Carver, C.S., Sutton, S.K., Scheier, M.F., 2000. Action, emotion, and personality: emerging conceptual integration. Pers. Soc. Psychol. Bull. 26, 741–751.

Chen, A.C., Liu, F.J., Wang, L., Arendt-Nielsen, L., 2006. Mode and site of acupuncture modulation in the human brain: 3D (124-ch) EEG power spectrum mapping and source imaging. Neuroimage 29, 1080–1091.

Chen, A.C., Feng, W., Zhao, H., Yin, Y., Wang, P., 2008. EEG default mode network in the human brain: spectral regional field powers. Neuroimage 41, 561–574.

Chiang, A.K., Rennie, C.J., Robinson, P.A., Roberts, J.A., Rigozzi, M.K., Whitehouse, R.W., et al., 2008. Automated characterization of multiple alpha peaks in multi-site electroencephalograms. J. Neurosci. Methods 168, 396–411.

Clark, C.R., Veltmeyer, M.D., Hamilton, R.J., Simms, E., Paul, R., Hermens, D., et al., 2004. Spontaneous alpha peak frequency predicts working memory performance across the age span. Int. J. Psychophysiol. 53, 1–9.

Comrey, A.L., Lee, H.B., 1992. A First Course in Factor Analysis, 2nd ed. LEA, Hillsdale, NJ.

Cortina, J.M., 1993. What is coefficient alpha? An examination of theory and applications. J. Appl. Psychol. 78, 98–104.

Crawford, H.J., Clarke, S.W., Kitner-Triolo, M., 1996. Self-generated happy and sad emotions in low and highly hypnotizable persons during waking and hypnosis: laterality and regional EEG activity differences. Int. J. Psychophysiol. 24, 239–266.

Darvas, F., Scherer, R., Ojemann, J.G., Rao, R.P., Miller, K.J., Sorensen, L.B., 2010. High gamma mapping using EEG. Neuroimage 49, 930–938.

Davidson, R.J., Chapman, J.P., Chapman, L.J., Henriques, J.B., 1990. Asymmetrical brain electrical activity discriminates between psychometrically-matched verbal and spatial cognitive tasks. Psychophysiology 27, 528–543.

Davidson, R.J., Jackson, D.C., Larson, C.L., 2000a. Human electroencephalography, In: Cacioppo, J.T., Tassinary, L.G., Berntson, G.G. (Eds.), Handbook of Psychophysiology, 2nd ed. Cambridge University Press, NY, pp. 27–52.

Davidson, R.J., Marshall, J.R., Tomarken, A.J., Henriques, J.B., 2000b. While a phobic waits: regional brain electrical and autonomic activity in social phobics during anticipation of public speaking. Biol. Psychiatry 47, 85–95.

Debener, S., Kayser, J., Tenke, C.E., Beauducel, A., 2000. Principal components analysis (PCA) as a tool for identifying EEG frequency bands: II. Dissociation of resting alpha asymmetries. Psychophysiology 37, S35.

Delorme, A., Sejnowski, T., Makeig, S., 2007a. Enhanced detection of artifacts in EEG data using higher-order statistics and independent component analysis. Neuroimage 34, 1443–1449.

Delorme, A., Westerfield, M., Makeig, S., 2007b. Medial prefrontal theta bursts precede rapid motor responses during visual selective attention. J. Neurosci. 27, 11949–11959.

Dien, J., 1998. Issues in the application of the average reference: review, critiques, and recommendations. Behav. Res. Methods Instrum. Comp. 30, 34–43.

Dien, J., 2010. Evaluating two-step PCA of ERP data with geomin, infomax, oblimin, promax, and varimax rotations. Psychophysiology 47, 170–183.

Dien, J., Beal, D.J., Berg, P., 2005. Optimizing principal components analysis of event-related potentials: matrix type, factor loading weighting, extraction, and rotations. Clin. Neurophysiol. 116, 1808–1825.

Donchin, E., Heffley, E., 1978. Multivariate analysis of event-related potential data: a tutorial review. In: Otto, D.A. (Ed.), Multidisciplinary Perspectives in Event-Related Brain Potential Research. US Environmental Protection Agency Office of Research and Development, Washington, DC, pp. 555–572.

Duffy, F.H., Jones, K., Bartels, P., McAnulty, G., Albert, M., 1992. Unrestricted principal components analysis of brain electrical activity: issues of data dimensionality, artifact, and utility. Brain Topogr. 4, 291–307.

Dustman, R.E., Shearer, D.E., Emmerson, R.Y., 1999. Life-span changes in EEG spectral amplitude, amplitude variability and mean frequency. Clin. Neurophysiol. 110, 1399–1409.

Edwards, E., Soltani, M., Kim, W., Dalal, S.S., Nagarajan, S.S., Berger, M.S., et al., 2009. Comparison of time–frequency responses and the event-related potential to auditory speech stimuli in human cortex. J. Neurophysiol. 102, 377–386.

Elliot, A.J., Thrash, T.M., 2002. Approach-avoidance motivation in personality: approach and avoidance temperament and goals. J. Pers. Soc. Psychol. 82, 804–818.

Everhart, D.E., Demaree, H.A., 2003. Low alpha power (7.5–9.5 Hz) changes during positive and negative affective learning. Cogn. Affect. Behav. Neurosci. 3, 39–45.

Everhart, D.E., Demaree, H.A., Wuensch, K.L., 2003. Healthy high-hostiles evidence low-alpha power changes during negative affect learning. Brain Cogn. 52, 334–342.

Everhart, D.E., Demaree, H.A., Harrison, D.W., 2008. The influence of hostility on electroencephalographic activity and memory functioning during an affective memory task. Clin. Neurophysiol. 119, 134–143.

Fabiani, M., Gratton, G., Karis, D., Donchin, E., 1987. Definition, identification, and reliability of measurement of the P300 component of the event-related brain potential. In: Ackles, P.K., Jennings, J.R., Coles, M.G.H. (Eds.), Advances in Psychophysiology, Vol. 2. JAI Press, Greenwich, CT, pp. 1–78.

Fava, J.L., Velicer, W.F., 1996. The effects of underextraction in factor and component analysis. Educ. Psychol. Meas. 56, 907–929.

Ferree, T.C., Brier, M.R., Hart Jr., J., Kraut, M.A., 2009. Space–time–frequency analysis of EEG data using within-subject statistical tests followed by sequential PCA. Neuroimage 45, 109–121.

Freeman, W.J., 1987. Analytic techniques used in the search for the physiological basis of the EEG. In: Gevins, A., Remond, A. (Eds.), Handbook of Electroencephalography and Clinical Neurophysiology, Vol. 3A. Elsevier, Amsterdam, pp. 583–664.

Freeman, W.J., Grajski, K.A., 1987. Relation of olfactory EEG to behavior: factor analysis. Behav. Neurosci. 101, 766–777.

Freunberger, R., Fellinger, R., Sauseng, P., Gruber, W., Klimesch, W., 2009. Dissociation between phase-locked and nonphase-locked alpha oscillations in a working memory task. Hum. Brain Mapp. 30, 3417–3425.

Gasser, T., Bacher, P., Mocks, J., 1982. Transformations towards the normal distribution of broad band spectral parameters of the EEG. Electroencephalography and Clinical Neurophysiology 53, 119–124.

Gasser, T., Ziegler, P., Gattaz, W.F., 1992. The deleterious effect of ocular artefacts on the quantitative EEG, and a remedy. Eur. Arch. Psychiatry Clin. Neurosci. 241, 352–356.

Gevins, A., Smith, M.E., McEvoy, L., Yu, D., 1997. High-resolution EEG mapping of cortical activation related to working memory: effects of task difficulty, type of processing, and practice. Cereb. Cortex 7, 374–385.

Gibbs, F.A., 1942. Cortical frequency spectra of healthy adults. J. Nerv. Ment. Dis. 95, 417–426.

Goncharova, I.I., Barlow, J.S., 1990. Changes in EEG mean frequency and spectral purity during spontaneous alpha blocking. Electroencephalogr. Clin. Neurophysiol. 76, 197–204.

Goncharova, I.I., Davidson, R.J., 1995. The factor structure of EEG—differential validity of low, high alpha power asymmetry in predicting affective style. Psychophysiology 32, S35.

Gorsuch, R.L., 1983. Factor Analysis, 2nd ed. LEA, Hillsdale, NJ.

Greischar, L.L., Burghy, C.A., van Reekum, C.M., Jackson, D.C., Pizzagalli, D.A., Mueller, C., et al., 2004. Effects of electrode density and electrolyte spreading in dense array electroencephalographic recording. Clin. Neurophysiol. 115, 710–720.

Guadagnoli, E., Velicer, W.F., 1988. Relation of sample size to the stability of component patterns. Psychol. Bull. 103, 265–275.

Gudmundsson, S., Runarsson, T.P., Sigurdsson, S., Eiriksdottir, G., Johnsen, K., 2007. Reliability of quantitative EEG features. Clin. Neurophysiol. 118, 2162–2171.

Hamidi, M., Slagter, H.A., Tononi, G., Postle, B.R., 2009. Repetitive transcranial magnetic stimulation affects behavior by biasing endogenous cortical oscillations. Front. Integr. Neurosci. 3, 14.

Harris, F.J., 1978a. On the use of windows for harmonic analysis with the discrete Fourier transform. Proc. IEEE 66, 51–83.

Harris, F.J., 1978b. On the use of windows for harmonic analysis with the discrete Fourier transform. Proc. IEEE 66, 51–83.

Hayes, A.F., Krippendorff, K., 2007. Answering the call for a standard reliability measure for coding data. Commun. Methods Measures 1, 77–89.

He, B.J., Snyder, A.Z., Zempel, J.M., Smyth, M.D., Raichle, M.E., 2008. Electrophysiological correlates of the brain's intrinsic large-scale functional architecture. Proc. Natl. Acad. Sci. U. S. A. 105, 16039–16044.

Henriques, J.B., Davidson, R.J., 1991. Left frontal hypoactivation in depression. J. Abnorm. Psychol. 100, 535–545.

Herrmann, C.S., Arnold, T., Visbeck, A., Hundemer, H.P., Hopf, H.C., 2001. Adaptive frequency decomposition of EEG with subsequent expert system analysis. Comput. Biol. Med. 31, 407–427.

Horn, J.L., 1965. A rationale and a test for the number of factors in factor analysis. Psychometrika 30, 179–185.

Hotelling, H., 1940. The selection of variates for use in prediction with some comments on the general problem of nuisance parameters. The Annals of Mathematical Statistics 11, 271–283.

Hyvarinen, A., Ramkumar, P., Parkkonen, L., Hari, R., 2010. Independent component analysis of short-time Fourier transforms for spontaneous EEG/MEG analysis. Neuroimage 49, 257–271.
Inanaga, K., 1998. Frontal midline theta rhythm and mental activity. Psychiatry Clin. Neurosci. 52, 555–566.
Jacobs, G.D., Snyder, D., 1996. Frontal brain asymmetry predicts affective style in men. Behav. Neurosci. 110, 3–6.
Jann, K., Dierks, T., Boesch, C., Kottlow, M., Strik, W., Koenig, T., 2009. BOLD correlates of EEG alpha phase-locking and the fMRI default mode network. Neuroimage 45, 903–916.
Karson, C.N., Coppola, R., Morihisa, J.M., Weinberger, D.R., 1987. Computed electroencephalographic activity mapping in schizophrenia. The resting state reconsidered. Arch. Gen. Psychiatry 44, 514–517.
Keren, A.S., Yuval-Greenberg, S., Deouell, L.Y., 2010. Saccadic spike potentials in gamma-band EEG: characterization, detection and suppression. Neuroimage 49, 2248–2263.
Kierkels, J.J., Riani, J., Bergmans, J.W., van Boxtel, G.J., 2007. Using an eye tracker for accurate eye movement artifact correction. IEEE Trans. Biomed. Eng. 54, 1256–1267.
Klimesch, W., 1999. EEG alpha and theta oscillations reflect cognitive and memory performance: a review and analysis. Brain Res. Brain Res. Rev. 29, 169–195.
Knott, V.J., 2001. Electroencephalographic characterization of cigarette smoking behavior. Alcohol 24, 95–97.
Knyazev, G.G., 2007. Motivation, emotion, and their inhibitory control mirrored in brain oscillations. Neurosci. Biobehav. Rev. 31, 377–395.
Knyazev, G.G., Slobodskoj-Plusnin, J.Y., Bocharov, A.V., 2009. Event-related delta and theta synchronization during explicit and implicit emotion processing. Neuroscience 164, 1588–1600.
Kramer, A.F., 1985. The interpretation of the component structure of event-related potentials: an analysis of expert judgments. Psychophysiology 22, 334–344.
Kubicki, S., Herrmann, W.M., Fichte, K., Freund, G., 1979. Reflections on the topics: EEG frequency bands and regulation of vigilance. Pharmakopsychiatr. Neuropsychopharmakol. 12, 237–245.
Kuhlo, W., 1976. The beta rhythms. In: Remond, A. (Ed.), Handbook of Electroencephalography and Clinical Neurophysiology, Vol. 6A. Elsevier, Amsterdam, pp. 89–104.
Lakatos, P., Karmos, G., Mehta, A.D., Ulbert, I., Schroeder, C.E., 2008. Entrainment of neuronal oscillations as a mechanism of attentional selection. Science 320, 110–113.
Larson, C.L., Davidson, R.J., Abercrombie, H.C., Ward, R.T., Schaefer, S.M., Jackson, D.C., et al., 1998. Relations between PET-derived measures of thalamic glucose metabolism and EEG alpha power. Psychophysiology 35, 162–169.
Lawrence, F.R., Hancock, G.R., 1999. Conditions affecting integrity of a factor solution under varying degrees of overextraction. Educ. Psychol. Meas. 59, 549–579.
Lee, T.W., Girolami, M., Sejnowski, T.J., 1999. Independent component analysis using an extended infomax algorithm for mixed subgaussian and supergaussian sources. Neural Comput. 11, 417–441.
Lehmann, D., 1971. Multichannel topography of human alpha EEG fields. Electroencephalogr. Clin. Neurophysiol. 31, 439–449.
Lobaugh, N.J., West, R., McIntosh, A.R., 2001. Spatiotemporal analysis of experimental differences in event-related potential data with partial least squares. Psychophysiology 38, 517–530.
Lopes da Silva, F., 2005. EEG analysis: theory and practice, In: Niedermeyer, E., Lopes da Silva, F. (Eds.), Electroencephalography. Basic Principles, Clinical Applications, and Related Fields, 5th ed. Lippincott Williams & Wilkins, Philadelphia, PA, pp. 1199–1231.
Makeig, S., Westerfield, M., Jung, T.P., Enghoff, S., Townsend, J., Courchesne, E., et al., 2002. Dynamic brain sources of visual evoked responses. Science 295, 690–694.
Makeig, S., Delorme, A., Westerfield, M., Jung, T.P., Townsend, J., Courchesne, E., et al., 2004. Electroencephalographic brain dynamics following manually responded visual targets. PLoS Biol. 2, e176.
Manning, J.R., Jacobs, J., Fried, I., Kahana, M.J., 2009. Broadband shifts in local field potential power spectra are correlated with single-neuron spiking in humans. J. Neurosci. 29, 13613–13620.
Mantini, D., Perrucci, M.G., Del Gratta, C., Romani, G.L., Corbetta, M., 2007. Electrophysiological signatures of resting state networks in the human brain. Proc. Natl. Acad. Sci. U. S. A. 104, 13170–13175.
Marcuse, L.V., Schneider, M., Mortati, K.A., Donnelly, K.M., Arnedo, V., Grant, A.C., 2008. Quantitative analysis of the EEG posterior-dominant rhythm in healthy adolescents. Clin. Neurophysiol. 119, 1778–1781.
Maris, E., Oostenveld, R., 2007. Nonparametric statistical testing of EEG- and MEG-data. J. Neurosci. Methods 164, 177–190.
Mathersul, D., Williams, L.M., Hopkinson, P.J., Kemp, A.H., 2008. Investigating models of affect: relationships among EEG alpha asymmetry, depression, and anxiety. Emotion 8, 560–572.
McIntosh, A.R., Lobaugh, N.J., 2004. Partial least squares analysis of neuroimaging data: applications and advances. Neuroimage 23, S250–S263.
McMenamin, B.W., Shackman, A.J., Maxwell, J.S., Greischar, L.L., Davidson, R.J., 2009. Validation of regression-based myogenic correction techniques for scalp and source-localized EEG. Psychophysiology 46, 578–592.
McMenamin, B.W., Shackman, A.J., Maxwell, J.S., Bachhuber, D.R.W., Koppenhaver, A. M., Greischar, L.L., et al., 2010. Validation of ICA-based myogenic artifact correction for scalp and source-localized EEG. Neuroimage 49, 2416–2432.
Mecklinger, A., Kramer, A.F., Strayer, D.L., 1992. Event related potentials and EEG components in a semantic memory search task. Psychophysiology 29, 104–119.
Meltzer, J.A., Negishi, M., Mayes, L.C., Constable, R.T., 2007. Individual differences in EEG theta and alpha dynamics during working memory correlate with fMRI responses across subjects. Clin. Neurophysiol. 118, 2419–2436.
Michel, C.M., Pascual-Marqui, R.D., Strik, W.K., Koenig, T., Lehmann, D., 1995. Frequency domain source localization shows state-dependent diazepam effects in 47-channel EEG. J. Neural Transm. 99, 157–171.
Mitchell, D.J., McNaughton, N., Flanagan, D., Kirk, I.J., 2008. Frontal-midline theta from the perspective of hippocampal "theta". Prog. Neurobiol. 86, 156.
Motokizawa, F., Fujimori, B., 1964. Fast activities and DC potential changes of the cerebral cortex during EEG arousal response. Electroencephalogr. Clin. Neurophysiol. 17, 630–637.
Murray, M.M., Brunet, D., Michel, C.M., 2008. Topographic ERP analyses: a step-by-step tutorial review. Brain Topogr. 20, 249–264.
Neuper, C., Pfurtscheller, G., 2001. Event-related dynamics of cortical rhythms: frequency-specific features and functional correlates. Int. J. Psychophysiol. 43, 41–58.
Nichols, T., 2007. False discovery rate procedures. In: Friston, K., Ashburner, J., Kiebel, S., Nichols, T., Penny, W. (Eds.), Statistical Parametric Mapping. The Analysis of Functional Brain Images. Elsevier, NY, pp. 246–252.
Nichols, T.E., Holmes, A.P., 2002. Nonparametric permutation tests for functional neuroimaging: a primer with examples. Hum. Brain Mapp. 15, 1–25.
Nichols, T., Holmes, A., 2007. Non-parametric procedures. In: Friston, K., Ashburner, J., Kiebel, S., Nichols, T., Penny, W. (Eds.), Statistical Parametric Mapping. The Analysis of Functional Brain Images. Elsevier, NY, pp. 253–274.
Niedermeyer, E., 2005. The normal EEG of the waking adult. In: Niedermeyer, E., Lopes da Silva, F.H. (Eds.), Electroencephalography: Basic Principles, Clinical Applications, and Related Fields. Lippincott, Williams & Wilkins, Philadelphia, PA, pp. 167–192.
Nunez, P.L., Srinivasan, R., 2005. Electric Fields of the Brain: The Neurophysics of EEG, 2nd ed. Oxford University Press, NY.
Nunez, P.L., Wingeier, B.M., Silberstein, R.B., 2001. Spatial–temporal structures of human alpha rhythms: theory, microcurrent sources, multiscale measurements, and global binding of local networks. Hum. Brain Mapp. 13, 125–164.
Nunnally, J.C., Bernstein, I.H., 1994. Psychometric Theory, 3rd ed. McGraw-Hill, NY.
Nuwer, M.R., Lehmann, D., da Silva, F.L., Matsuoka, S., Sutherling, W., Vibert, J.F., 1999. IFCN guidelines for topographic and frequency analysis of EEGs and EPs. The International Federation of Clinical Neurophysiology. Electroencephalogr. Clin. Neurophysiol. (Supplement) 52, 15–20.
Oakes, T.R., Pizzagalli, D.A., Hendrick, A.M., Horras, K.A., Larson, C.L., Abercrombie, H.C., et al., 2004. Functional coupling of simultaneous electrical and metabolic activity in the human brain. Hum. Brain Mapp. 21, 257–270.
Ojemann, G.A., Corina, D.P., Corrigan, N., Schoenfield-McNeill, J., Poliakov, A., Zamora, L., et al., 2010. Neuronal correlates of functional magnetic resonance imaging in human temporal cortex. Brain 133 (Pt 1), 46–59.
Okada, S., Urakami, Y., 1993. Midline theta rhythm revisited. Clin. Electroencephalogr. 24, 6–12.
Onton, J., Delorme, A., Makeig, S., 2005. Frontal midline EEG dynamics during working memory. Neuroimage 27, 341–356.
Onton, J., Westerfield, M., Townsend, J., Makeig, S., 2006. Imaging human EEG dynamics using independent component analysis. Neurosci. Biobehav. Rev. 30, 808–822.
Palmer, F.B., Yarworth, S., Niedermeyer, E., 1976. Frontal midline theta rhythm. Clin. Electroencephalogr. 7, 131–138.
Palva, S., Palva, J.M., 2007. New vistas for alpha-frequency band oscillations. Trends Neurosci. 30, 150–158.
Papousek, I., Schulter, G., 2001. Associations between EEG asymmetries and electrodermal lability in low vs. high depressive and anxious normal individuals. Int. J. Psychophysiol. 41, 105–117.
Pascual-Marqui, R.D., Lehmann, D., Koenig, T., Kochi, K., Merlo, M.C.G., Hell, D., et al., 1999. Low resolution brain electromagnetic tomography (LORETA) functional imaging in acute, neuroleptic-naive, first-episode, productive schizophrenia. Psychiatry Res. Neuroimaging 90, 169–179.
Peres-Neto, P.R., Jackson, D.A., Somers, K.M., 2005. How many principal components? Stopping rules for determining the number of non-trivial axes revisited. Comput. Stat. Data Anal. 49, 974–997.
Petruzzello, S.J., Landers, D.M., 1994. State anxiety reduction and exercise: does hemispheric activation reflect such changes? Med. Sci. Sports Exerc. 26, 1028–1035.
Pizzagalli, D.A., Oakes, T.R., Fox, A.S., Chung, M.K., Larson, C.L., Abercrombie, H.C., et al., 2004. Functional but not structural subgenual prefrontal cortex abnormalities in melancholia. Mol. Psychiatry 9 (325), 393–405.
Poolman, P., Frank, R.M., Luu, P., Pederson, S.M., Tucker, D.M., 2008. A single-trial analytic framework for EEG analysis and its application to target detection and classification. Neuroimage 42, 787–798.
Raghavachari, S., Kahana, M.J., Rizzuto, D.S., Caplan, J.B., Kirschen, M.P., Bourgeois, B., et al., 2001. Gating of human theta oscillations by a working memory task. J. Neurosci. 21, 3175–3183.
Rihs, T.A., Michel, C.M., Thut, G., 2009. A bias for posterior alpha-band power suppression versus enhancement during shifting versus maintenance of spatial attention. Neuroimage 44, 190–199.
Ritter, P., Moosmann, M., Villringer, A., 2009. Rolandic alpha and beta EEG rhythms' strengths are inversely related to fMRI-BOLD signal in primary somatosensory and motor cortex. Hum. Brain Mapp. 30, 1168–1187.
Rosa, J., Kilner, J., Blankenburg, F., Josephs, O., Penny, W., 2010. Estimating the transfer function from neuronal activity to BOLD using simultaneous EEG-fMRI. Neuroimage 49, 1496–1509.
Sakamoto, S., Tanaka, H., Tsuyuguchi, N., Terakawa, Y., Ohata, K., Inoue, Y., et al., 2010. Quantitative imaging of spontaneous neuromagnetic activity for assessing cerebral ischemia using sLORETA-qm. Neuroimage 49, 488–497.
Sammer, G., Blecker, C., Gebhardt, H., Bischoff, M., Stark, R., Morgen, K., et al., 2007. Relationship between regional hemodynamic activity and simultaneously recorded EEG-theta associated with mental arithmetic-induced workload. Hum. Brain Mapp. 28, 793–803.

Schacter, D.L., 1977. EEG theta waves and psychological phenomena: a review and analysis. Biol. Psychol. 5, 47–82.
Schroeder, M.J., Barr, R.E., 2000. An alpha modulation index for electroencephalographic studies using complex modulation. Med. Biol. Eng. Comput. 38, 306–310.
Shackman, A.J., 2010. The potentially deleterious impact of muscle activity on gamma band inferences. Neuropsychopharmacology 35, 847.
Shackman, A.J., McMenamin, B.W., Maxwell, J.S., Greischar, L.L., Davidson, R.J., 2009a. Right dorsolateral prefrontal cortical activity and behavioral inhibition. Psychol. Sci. 20, 1500–1506.
Shackman, A.J., McMenamin, B.W., Slagter, H.A., Maxwell, J.S., Greischar, L.L., Davidson, R.J., 2009b. Electromyogenic artifacts and electroencephalographic inferences. Brain Topogr. 21, 7–12.
Shaw, J.C., 2003. The Brain's Alpha Rhythms and the Mind. Elsevier, NY.
Smit, D.J.A., Posthuma, D., Boomsma, D.I., Geus, E.J., 2005. Heritability of background EEG across the power spectrum. Psychophysiology 42, 691–697.
Steinvorth, S., Wang, C., Ulbert, I., Schomer, D., Halgren, E., 2010. Human entorhinal gamma and theta oscillations selective for remote autobiographical memory. Hippocampus 20, 166–173.
Stewart, J.L., Levin-Silton, R., Sass, S.M., Heller, W., Miller, G.A., 2008. Anger style, psychopathology, and regional brain activity. Emotion 8, 701–713.
Sutton, S.K., Davidson, R.J., 1997. Prefrontal brain asymmetry: a biological substrate of the behavioral approach and inhibition systems. Psychol. Sci. 8, 204–210.
Takahashi, N., Shinomiya, S., Mori, D., Tachibana, S., 1997. Frontal midline theta rhythm in young healthy adults. Clin. Electroencephalogr. 28, 49–54.
Tenke, C.E., Kayser, J., 2005. Reference-free quantification of EEG spectra: combining current source density (CSD) and frequency principal components analysis (fPCA). Clin. Neurophysiol. 116, 2826–2846.
ter Braak, C.J.F., 1992. Permutation versus bootstrap significance tests in multiple regression and ANOVA. Bootstrapping and related techniques. In: Jockel, K.-H., Rothe, G., Sendler, W. (Eds.), Bootstrapping and Related Techniques. Springer-Verlag, Berlin, pp. 79–86.
Thibodeau, R., Jorgensen, R.S., Kim, S., 2006. Depression, anxiety, and resting frontal EEG asymmetry: a meta-analytic review. J. Abnorm. Psychol. 115, 715–729.
Tomarken, A.J., Davidson, R.J., 1994. Frontal brain activation in repressors and nonrepressors. J. Abnorm. Psychol. 103, 339–349.
Tomarken, A.J., Davidson, R.J., Henriques, J.B., 1990. Resting frontal brain asymmetry predicts affective responses to films. J. Pers. Soc. Psychol. 59, 791–801.
Tomarken, A.J., Davidson, R.J., Wheeler, R.E., Doss, R.C., 1992a. Individual differences in anterior brain asymmetry and fundamental dimensions of emotion. J. Pers. Soc. Psychol. 62, 676–687.
Tomarken, A.J., Davidson, R.J., Wheeler, R.E., Kinney, L., 1992b. Psychometric properties of resting anterior EEG asymmetry: temporal stability and internal consistency. Psychophysiology 29, 576–592.
Tsujimoto, T., Shimazu, H., Isomura, Y., Sasaki, K., 2010. Theta oscillations in primate prefrontal and anterior cingulate cortices in forewarned reaction time tasks. J. Neurophysiol. 103, 827–843.
Uhlhaas, P.J., Singer, W., 2010. Abnormal neural oscillations and synchrony in schizophrenia. Nat. Rev. Neurosci. 11, 100–113.
Van Albada, S.J., Rennie, C.J., Robinson, P.A., 2007. Variability of model-free and model-based quantitative measures of EEG. J. Integr. Neurosci. 6, 279–307.
van Albada, S.J., Kerr, C.C., Chiang, A.K., Rennie, C.J., Robinson, P.A., 2010. Neurophysiological changes with age probed by inverse modeling of EEG spectra. Clin. Neurophysiol. 121, 21–38.
Varmuza, K., Filzmoser, P., 2009. Introduction to Multivariate Statistical Analysis in Chemometrics. CRC Press, NY.
Velicer, W.F., Eaton, C.A., Fava, J.L., 2000. Construct explication through factor or component analysis: a review and evaluation of alternative procedures for determining the number of factors or components. In: Goffin, R.D., Helms, E. (Eds.), Problems and Solutions in Human Assessment. : Honoring Douglas N. Jackson at Seventy. Springer, Norwell, MA, pp. 41–71.
Volavka, J., Matousek, J., Roubicek, J., 1967. Mental arithmetic and eye opening. Electroencephalogr. Clin. Neurophysiol. 22, 174–176.
Wacker, J., Heldmann, M., Stemmler, G., 2003. Separating emotion and motivational direction in fear and anger: effects on frontal asymmetry. Emotion 3, 167–193.
Wacker, J., Dillon, D.G., Pizzagalli, D.A., 2009. The role of the nucleus accumbens and rostral anterior cingulate cortex in anhedonia: integration of resting EEG, fMRI, and volumetric techniques. Neuroimage 46, 327–337.
Wang, C., Ulbert, I., Schomer, D.L., Marinkovic, K., Halgren, E., 2005. Responses of human anterior cingulate cortex microdomains to error detection, conflict monitoring, stimulus-response mapping, familiarity, and orienting. J. Neurosci. 25, 604–613.
Welch, P., 1967. The use of fast Fourier transform for the estimation of power spectra: a method based on time averaging over short, modified periodograms. IEEE Trans. Audio Electroacoustics 15, 70–73.
Westmoreland, B.F., Klass, D.W., 1986. Midline theta rhythm. Arch. Neurol. 43, 139–141.
Westmoreland, B.F., Klass, D.W., 1990. Unusual EEG patterns. J. Clin. Neurophysiol. 7, 209–228.
Wheeler, R.E., Davidson, R.J., Tomarken, A.J., 1993. Frontal brain asymmetry and emotional reactivity: a biological substrate of affective style. Psychophysiology 30, 82–89.
Whitham, E.M., Lewis, T., Pope, K.J., Fitzgibbon, S.P., Clark, C.R., Loveless, S., et al., 2008. Thinking activates EMG in scalp electrical recordings. Clin. Neurophysiol. 119, 1166–1175.
Whittingstall, K., Logothetis, N.K., 2009. Frequency-band coupling in surface EEG reflects spiking activity in monkey visual cortex. Neuron 64, 281–289.
Womelsdorf, T., Johnston, K.M., Vinck, M., Everling, S., 2010. Theta-activity in anterior cingulate cortex predicts task rules and their adjustments following errors. Proc. Natl. Acad. Sci. U. S. A. 107, 5248–5253.
Wood, J.M., Tataryn, D.J., Gorsuch, R.L., 1996. Effects of under- and overextraction on principal axis factor analysis with varimax rotation. Psychol. Methods 1, 354–365.
Woodward, T.S., Cairo, T.A., Ruff, C.C., Takane, Y., Hunter, M.A., Ngan, E.T.C., 2006. Functional connectivity reveals load dependent neural systems underlying encoding and maintenance in verbal working memory. Neuroscience 139, 317–325.
Wyart, V., Tallon-Baudry, C., 2008. Neural dissociation between visual awareness and spatial attention. J. Neurosci. 28, 2667–2679.
Wyczesany, M., Kaiser, J., Coenen, A.M., 2008. Subjective mood estimation co-varies with spectral power EEG characteristics. Acta Neurobiol. Exp. 68, 180–192.
Yuval-Greenberg, S., Tomer, O., Keren, A.S., Nelken, I., Deouell, L.Y., 2008. Transient induced gamma-band response in EEG as a manifestation of miniature saccades. Neuron 58, 429–441.
Zeman, P.M., Till, B.C., Livingston, N.J., Tanaka, J.W., Driessen, P.F., 2007. Independent component analysis and clustering improve signal-to-noise ratio for statistical analysis of event-related potentials. Clin. Neurophysiol. 118, 2591–2604.
Zwick, W.R., Velicer, W.F., 1986. Comparison of five rules for determining the number of components to retain. Psychol. Bull. 99, 432–442.

Identifying Robust and Sensitive Frequency Bands for Interrogating Neural Oscillations: *Supplementary Method and Results*

AJ Shackman, BW McMenamin, JS Maxwell, LL Greischar & RJ Davidson

Contents

Spectral Factor Analysis (SFA)

SFA entails three conceptually distinct steps:

1. *Factor extraction*.

SFA can be performed using either the correlation or covariance matrix formed by the power at each frequency. In the case of the correlation matrix, R, it can be shown that $R = (VL^{1/2}) \times (L^{1/2}V')$, where V is the matrix of *eigenvectors*, the weighted linear combination of measured variables, and L is the diagonal matrix of *eigenvalues*, the variance accounted for by each eigenvector (Gorsuch, 1983; Harman, 1976). For correlation matrices of full rank, the number of eigenvectors and eigenvalues is equal to the number of measured variables. $VL^{1/2}$ is equal to Λ, the unrotated matrix of *loadings* (i.e., weights), the correlations between the measured variables and latent factors. In practice, V and L are often solved using principal component analysis (PCA; i.e., the Karhunen-Loève transform) or maximum likelihood. For PCA, the first eigenvector maximizes the predicted variance using ordinary least squares. Each successive eigenvector maximizes the predicted residual variance. For spectral factor analysis (SFA), variance is typically across individuals, although additional measurement categories are commonly incorporated (e.g., conditions, electrodes).

Although SFA can be performed using the correlation or covariance matrix, the covariance matrix will bias the solution toward the frequencies and electrodes with maximal variance. For the tonic (i.e., resting) EEG, this means that the resulting band definitions will emphasize the contribution of posterior channels and frequencies in the alpha range (see Figure 1 in the main report), to the detriment of other regions of the scalp and spectrum. Whereas this is considered problematic for SFAs of the tonic EEG (Arruda et al., 1996), it can be useful in cases where the aim is to define bands sensitive to regional differences in spectral activation across conditions. Indeed, the covariance matrix is generally recommended for event-related potential (ERP) studies because it tends to yield greater fidelity with the raw waveforms than the correlation matrix (Dien, *in press-a;* Donchin & Heffley, 1978; Kayser & Tenke, 2006). Freely available Matlab code optimized for use with ERP datasets is available for this purpose (http://sourceforge.net/projects/erppcatoolkit; http://psychophysiology.cpmc.columbia.edu/software/index.html). Along similar lines, the covariance matrix has also been adopted for analyses in the time-frequency domain (Bernat, Williams, & Gehring, 2005; Ferree, Brier, Hart, & Kraut, 2009).

2. *Factor retention*.

The number of factors required to adequately reproduce the observed data is identified and minor factors are discarded. Minor factors include those accounting for trivial amounts of variance (e.g., eigenvalue < 1) or defined by an insufficient number of strong loadings (Zwick & Velicer, 1986). Retaining too few factors can lead to the artificial fusion of bands (Fava & Velicer, 1996), whereas retaining too many factors can produce artificial splitting, creating narrow bands at the expense of broader genuine ones (Lawrence & Hancock, 1999; Wood, Tataryn, & Gorsuch, 1996).

3. *Factor rotation and formation of bands*

To maximize factor simplicity and aid interpretability, the loadings relating the measured variables to the factors are rotated. Rotation amplifies strong factor loadings and suppresses weak ones. Rotation is accomplished by multiplying Λ by a transformation matrix, T. In the case of varimax (i.e., orthogonal) rotation, T is computed by maximizing the variance of the

squared normalized loadings across a factor. Loadings are normalized by their *communalities*, the proportion of its variance predicted by the factors, computed as the squared multiple correlation of the measured variable predicted by the factors.

In the case of SFA, the activity at each frequency can be transformed into formal bands by applying a threshold to the rotated factor loadings. In the present study, bands were formed on the basis of bins with loadings ≥.60, a value conventionally described as "good" to "very good" (Comrey & Lee, 1992). This stemmed from our aim of assessing whether the alpha sub-bands identified by SFA differ in their robustness and sensitivity. Use of a less stringent threshold would have increased the number of frequencies that loaded onto multiple factors (i.e., adjacent bands), increasing the degree of statistical dependence across sub-bands, and reducing the likelihood that they would differ. In general practice, we concur with suggestions that it is reasonable for contiguous bands to share border frequencies (Babiloni et al., 2007). Regardless, exploratory analyses (not reported) indicated that lowering this threshold somewhat did not alter our key conclusions. Suprathreshold bins were equally weighted, in keeping with common EEG practice (i.e., $\mu V^2/Hz$). The decision to eschew loading-weighted bands, which are typical of the ERP literature (e.g., Dien, *in press-b*), is unlikely to have had much impact: simulation studies indicate that unit-weighted (i.e., "rectangular windowed") and loading-weighted factor scores are highly correlated (Fava & Velicer, 1992). Unit-weighted bands also permit direct comparisons across samples (Floyd & Widaman, 1995).

BIS/BAS Questionnaire

Participants from the primary sample completed the seven-item *Behavioral Inhibition System* and thirteen-item *Behavioral Activation System* (BIS/BAS; Carver & White, 1994) scales. The BIS and BAS were designed to index sensitivity to punishment and reward, respectively. BIS items include *I feel worried when I think I have done poorly at something* and *Even if something bad is about to happen to me, I rarely experience fear or nervousness* [reverse-scored]). BAS items include *When I go after something, I use a 'no holds barred' approach* and *When good things happen to me, it affects me strongly*. Internal-consistency and test-retest reliability of the BIS/BAS is good, αs and *r*s > 0.66.

As we previously reported (Shackman, McMenamin, Maxwell, Greischar, & Davidson, 2009), the mean and variance of BIS scores (M = 19.3, SD = 2.9) was comparable to prior EEG studies (Coan & Allen, 2004), whereas they were somewhat smaller than previous reports for BAS (M = 40.5, SD = 3.8). BIS and BAS were uncorrelated, $r(49) = -0.09$, $p > 0.50$.

Reliability Analyses

It is widely believed that *reliability* places an upper limit on *sensitivity*. Sensitivity can refer to the power to detect either mean differences (e.g., across conditions or groups) or individual differences (i.e., predictive, concurrent, or criterion validity; Cronbach & Meehl, 1955). Indeed, classical measurement theory indicates that the upper bound of a metric's sensitivity is the square-root of the product of its own reliability and that of the signal, scale, or behavior that it is intended to predict (Nunnally & Bernstein, 1994). But it is important to realize that this is not necessarily true for the most commonly employed *psychometric* indices of reliability. In particular, it is possible for a metric to exhibit high sensitivity to individual differences despite low internal-consistency reliability (i.e., consistency across the measures or "items" comprising an aggregate metric; Rosenthal & Rosnow, 1991) or test-retest reliability (i.e., consistency across measurement occasions; Loevinger, 1957). Increases in internal-consistency reliability can be accompanied by decreased sensitivity to individual differences in multi-factorial constructs, such as depression, owing to increased redundancy of the constituent measures (i.e., insufficient content validity; Clark & Watson, 1995; Cronbach, 1960; Hogan & Roberts, 1996). And metrics can show exquisite sensitivity to mean differences in the face of low psychometric reliability (Lee, Shackman, Jackson, & Davidson, 2009; Zimmerman & Williams, 1986; Zimmerman, Williams, & Zumbo, 1993).

This begs the question, *What good is psychometric reliability?* The answer depends on whether one is interested in mean or individual differences. In the case of mean differences, relations between psychometric reliability and statistical power are complex (Zimmerman & Williams, 1986). The power of a mean difference test is an inverse function of the observed variance. Assuming that the "true" variance is constant, power monotonically *increases* with reliability because such increases can only be achieved by reducing the contribution of random error to observed variance (Total – True = Error; True = Observed Variance × Reliability). But if random error is constant, power monotonically *decreases* with reliability. Although the proportion of random error is not directly knowable in classical measurement theory, in both cases two or more metrics (e.g., EEG frequency bands) will differ in their statistical power as a function of both observed variance and psychometric reliability (Davidson, Chapman, Chapman, & Henriques, 1990; Melinder, Barch, Heydebrand, & Csernansky, 2005; Shackman et al., 2006). If one is interested in the sensitivity of a time-varying signal (e.g., event-related potentials), psychometric reliability is less informative than indices, such as the signal-to-noise ratio (SNR = mean / variance = coefficient of variation^{-1}), that scale monotonically with power (Handy, 2005; Huettel, Singerman, & McCarthy, 2001; Mocks, Gasser, & Kohler, 1988; Parrish, Gitelman, LaBar, & Mesulam, 2000) and the amount of aggregation (Luck, 2005) given random error and a stationary signal (Cacace & McFarland, 2003; Guilford, 1954; Rosenthal & Rosnow, 1991; Strube & Newman, 2007).

In the case of individual differences, statistical power is directly proportional to true variance (Chapman & Chapman, 1973, 1978, 2001). Increases in true variance permit finer discriminations (i.e., ranking) of individuals, whereas decreases (e.g., floor or ceiling effects) constrain the resolution of ranking. Although there are circumstances that violate the assumptions underlying this principle, it is likely to hold in the present study, where it seems reasonable to conceptualize the metrics that we wished to compare (factor analytically derived EEG frequency bands) and the construct they purportedly measure (alpha-like neurogenic activity) as one-dimensional. The implication for the present study is that variation in psychometric reliability is potentially informative about the cause of observed differences in sensitivity to individual differences across alpha bands. Because no such differences were obtained (see main report), reliability analyses are presented here primarily as a reference for future researchers.

Supplementary Table 1 (see below) presents the internal-consistency reliability across frequencies, indexed by Cronbach's coefficient α, for both conventional and SFA-defined alpha bands for the primary sample. Estimates and 95% confidence intervals (CIs) are provided for the grand average (i.e., collapsed across channels and blocks) and several representative channels (Fz and POz).

Pairwise contrasts for dependent coefficients (Feldt, Woodruff, & Salih, 1987) yielded several key findings. First, the use of conventional alpha sub-bands did not reduce reliability compared to broadband alpha, despite halving the number of constituent frequencies, a key determinant of coefficient α (Nunnally & Bernstein, 1994). Indeed, alpha-low was more reliable than broadband alpha at all channels examined, ts(49) < -2.92, ps < .006. There was no difference between the conventional alpha and alpha-high bands, ps > .75.

Second, a similar, but somewhat less clear pattern emerged for the SFA-defined sub-bands. Alpha-low was associated with increased reliability compared to broadband alpha for the grand average and Fz, *t*s(49) < -3.27, *p*s < .002. The difference was not significant for POz, $p = .12$. There was no difference between SFA-defined alpha-high and broadband alpha for the grand average and Fz, *p*s > .52. In the case of POz, SFA-defined alpha-high showed reduced reliability, $t(49) = 2.38$, $p = .02$.

Third, comparison of the conventional and SFA-defined alpha sub-bands revealed only isolated differences. Reliability was greater for SFA-defined alpha-low at Fz, $t(49) = -3.05$, $p = .004$. But the reverse pattern was obtained for alpha-high at POz, $t(49) = 2.48$, $p = .02$. None of the contrasts for the grand average or any of the other contrasts was significant, *p*s > .16.

Fourth, the conventional alpha sub-bands (i.e., low vs. high) did not differ in their reliability, *p*s > .20, whereas those defined by SFA did, *t*s(49) > 2.66, *p*s < .02. Specifically, the alpha-high sub-band was consistently less reliable than the alpha-low sub-band. The lower reliability of SFA-defined alpha-high did not appear to be an artifact of the small number of constituent frequencies (Nunnally & Bernstein, 1994). When we lowered the threshold to yield an alpha-high band ranging from 9 to 12 Hz (i.e., loadings ≥.50,), internal-consistency reliabilities were still relatively low (αs < .61 at the representative channels). By contrast, when we raised the threshold for alpha-low to produce a 2Hz-wide band (7-8Hz), reliabilities remained high, (αs > .89). Exploratory analyses (not reported) indicated that inclusion or exclusion of the peak alpha frequency (9Hz) had minimal consequences for the reliability of either SFA-defined sub-band.

Finally, it is worth noting that the non-alpha bands identified using SFA displayed excellent reliability, αs > .88 at the representative channels. Taken with our other results, this indicates that nearly all of the SFA-derived bands consistently exhibited adequate to excellent internal-consistency reliability.[1] The clear exception was the SFA-derived alpha-high band, which displayed lower and more topographically variable reliability.

Analyses of internal-consistency reliability for the secondary sample were broadly consistent with the larger primary sample. For the grand average (i.e., collapsed across channels and conditions), internal-consistency reliability of the SFA-derived alpha-low (α = .83, 95% CI: .65-.93) and alpha-high (α = .86, 95% CI: .61-.95) bands was good. The reliability of the conventional alpha (α = .76, 95% CI: .47-91) and alpha-low (α = .76, 95% CI: .47-.91) bands was also adequate. The reliability of the conventional alpha-high band was again lower (α = .48, 95% CI: -.15-.80).

[1] In accord with prior EEG research (Maltez, Hyllienmark, Nikulin, & Brismar, 2004; Tomarken, Davidson, Wheeler, & Kinney, 1992; Towers & Allen, 2009; Van Albada, Rennie, & Robinson, 2007), we also computed internal-consistency reliability *across blocks* for each of the conventional and SFA-defined bands separately for each channel. Reliability was uniformly excellent, αs > .97.

Supplementary Table 1. Mean Internal-Consistency Reliability (95% CIs) Across Frequencies for Different Alpha Band Definitions

Conventional Alpha 8-13 Hz (Range: .62 - .89)[a]	
Grand Average	.71 (.56 - .82)
Fz	.71 (.57 - .82)
POz	.69 (.54 - .81)
Conventional Alpha-Low 8-10 Hz (Range: .63 - .89)[a]	
Grand Average	.79 (.66 - .81)
Fz	.78 (.66 - .87)
POz	.77 (.64 - .86)
Conventional Alpha-High 11-13 Hz (Range: .55 - .97)[a]	
Grand Average	.73 (.58 - .84)
Fz	.71 (.54 - .83)
POz	.69 (.50 - .81)
SFA-Defined Alpha-Low 6-9Hz (Range: .70 - .93)[a]	
Grand Average	.83 (.74 - .90)
Fz	.86 (.78 - .91)
POz	.76 (.65 - .86)
SFA-Defined Alpha-High 10-11 Hz (Range: .50 - .92)[a]	
Grand Average	.67 (.42 - .81)
Fz	.71 (.48 - .83)
POz	.51 (.15 - .72)

[a] Range is across 129 channels (aggregated across blocks). Cronbach's α was computed using the grand average of the data matrix (*n* = 51 cases / band). Exploratory analyses (not reported) indicated a similar pattern of results when estimates were computed using the disaggregated matrix.

Supplementary Table 2. *Correlation Matrix for the Lower Frequencies*[a]

Hz	*1*	*2*	*3*	*4*	*5*	*6*	*7*	*8*	*9*	*10*	*11*	*12*	*13*	*14*	*15*	*16*	*17*	*18*	*19*	*20*	*21*	*21*	*22*	*23*	*24*
2	.91																								
3	.80	.88																							
4	.70	.79	.89																						
5	.55	.64	.74	.86																					
6	.42	.50	.60	.75	.86																				
7	.22	.30	.39	.56	.66	.81																			
8	.13	.18	.26	.41	.51	.68	.85																		
9	.08	.11	.15	.26	.33	.47	.57	**.78**																	
10	.07	.10	.13	.19	.22	.28	.34	**.47**	**.67**																
11	.11	.15	.18	.24	.27	.30	.30	**.37**	**.50**	**.78**															
12	.23	.27	.34	.39	.39	.42	.37	**.39**	**.47**	**.63**	**.79**														
13	.28	.32	.38	.44	.44	.48	.41	**.40**	**.42**	**.49**	**.63**	**.89**													
14	.30	.34	.42	.48	.49	.55	.48	.44	.43	.41	.53	.78	.89												
15	.29	.33	.42	.49	.50	.56	.51	.47	.43	.35	.45	.68	.80	.91											
16	.28	.32	.42	.49	.50	.56	.51	.49	.46	.36	.44	.64	.76	.86	.92										
17	.28	.31	.40	.47	.48	.53	.49	.52	.51	.40	.46	.63	.72	.82	.88	.92									
18	.26	.30	.39	.44	.45	.51	.46	.53	.59	.44	.47	.61	.67	.76	.81	.86	.92								
19	.24	.28	.36	.41	.40	.44	.39	.45	.58	.47	.47	.57	.62	.68	.72	.78	.85	.92							
20	.24	.28	.35	.38	.36	.37	.31	.36	.49	.47	.48	.56	.58	.62	.66	.72	.80	.87	.93						
21	.28	.31	.38	.38	.35	.33	.25	.27	.34	.39	.43	.52	.56	.60	.62	.69	.76	.81	.86	.91					
21	.30	.32	.38	.37	.33	.30	.21	.20	.23	.26	.35	.45	.50	.55	.58	.64	.71	.74	.78	.84	.92				
22	.32	.35	.39	.37	.32	.27	.17	.15	.16	.18	.26	.39	.46	.51	.54	.60	.66	.68	.71	.78	.89	.94			
23	.33	.35	.39	.36	.30	.25	.15	.12	.12	.12	.19	.34	.41	.46	.50	.55	.60	.63	.66	.72	.84	.90	.94		
24	.34	.35	.37	.34	.28	.23	.13	.10	.09	.09	.16	.31	.38	.44	.47	.53	.58	.60	.63	.69	.82	.89	.93	.95	

[a] Conventional alpha band (8 – 13 Hz) denoted by bold type. The correlation matrix was computed for 52,632 cases (51 *participants x* 129 *channels x* 8 *blocks*) and served as the input to the primary SFA. The first half of the matrix is presented here for descriptive purposes. Frequencies are rounded to the nearest integer.

Supplementary Table 3. *Correlations Among Alpha Bands for the Primary and Secondary Samples*[a]

		A Priori Defined			SFA Defined	
		Broad	Alpha-Low	Alpha-High	Alpha-Low	Alpha-High
A Priori	Broad	-	.99	.57	.89	.74
	Alpha-Low	.89	-	.45	.93	.66
	Alpha-High	.66	.26	-	.27	.80
SFA	Alpha-Low	.72	.92	.02	-	.38
	Alpha-High	.86	.62	.81	.31	-

[a] Correlations were computed using the grand average (i.e., aggregated across electrodes). The coefficients for Samples 1 (n = 51) and 2 (n = 17) are shown above and below the diagonal, respectively. Exploratory analyses (not reported) revealed a broadly similar pattern when correlations were computed using the complete data matrix (cases = participants × channels × blocks). Correlations among midfrontal asymmetry scores derived from these bands are described in the main report.

Supplementary Table 4. *SFA-Defined EEG Bands for the Primary and Secondary Samples.*[a]

						Extracted		*Rotated*				
Sample	Artifact Processing	Region (Number of Channels)	Number of Factors	Rotation	Factor Rank	Eigenvalue	Variance (%)	Eigenvalue	Variance (%)	Peak Loading (Hz)	Band[b] (Hz)	Prospective Label
1	Rejection	All (129)	5	Varimax	3	3.2	6.4	4.6	9.2	.91 (2)	1 - 5	Delta
					4	1.5	3.0	3.2	6.3	.86 (8)	6 - 9	Alpha-Low
					5	1.2	2.4	2.3	4.7	.85 (10)	10 - 11	Alpha-High
					2	8.5	17.0	7.8	15.6	.88 (14)	12 - 19	Beta
					1	30.2	60.5	26.8	53.5	.96 (40)	21 - 49	Gamma
2	ICA, Minimal	All (129)	5	Varimax	4	2.1	4.2	4.8	9.5	.93 (2)	1 - 5	Delta
					5	1.3	2.6	4.5	9.0	.94 (8)	6 - 9	Alpha-Low
					2	10.2	20.3	5.1	10.2	.78 (11)	10 - 11	Alpha-High
											19 - 21	Beta (Harmonic)
					3	3.6	7.1	5.1	10.1	.94 (13)	12 - 15	Beta
					1	28.4	56.9	26.1	52.2	.98 (45)	22 - 49	Gamma
2	ICA, Maximal	All (129)	5	Varimax	3	3.7	7.4	8.6	17.2	.93 (8)	2 - 9	Alpha-Low
					4	1.4	2.7	7.2	14.4	.82 (10)	10 - 11	Alpha-High
											19 - 21	Beta (Harmonic)
					2	5.7	11.3	8.7	17.4	.94 (13)	12 - 15	Beta
											22 - 25	Beta (Harmonic)
					5	1.0	2.1	1.6	3.2	none	n / a	n / a
					1	34.9	69.8	20.6	41.2	.97 (48)	27 - 49	Gamma
2	ICA, Maximal	All (129)	4	Varimax	3	3.7	7.4	8.4	16.8	.93 (8)	2 - 9	Alpha-Low
					4	1.4	2.7	8.0	16.1	.81 (11)	10 - 11	Alpha-High
											19 - 21	Beta (Harmonic)
					2	5.7	11.3	8.5	17.1	.94 (13)	12 - 15	Beta
											22 – 25	
					1	34.9	69.8	20.6	41.3	.93 (48)	27 - 49	Gamma

[a] Blocks were collapsed according to condition (eyes-open/closed) and the resulting matrix submitted to SFA. [b] Based on adjacent frequencies with rotated loadings ≥.60. Note: In order to explore the utility of using the covariance matrix for "activation" studies, additional SFAs were performed on the secondary sample paired with minimal ICA-based artifact correction. Four or five factors were extracted, varimax rotated, and thresholded. The five-factor solution yielded three bands with two or more suprathreshold loadings: delta (1-3Hz), alpha-low (5-9Hz), and alpha-high (12-15Hz). The four-factor solution yielded: delta (1-3Hz), alpha-low (6-9Hz), alpha-high (10-11Hz), and alpha-high/beta (11-14Hz). In both cases, solutions were biased toward the high-variance lower frequencies; low-variance upper frequencies failed to cohere into identifiable bands. The broad similarity of the solutions obtained for the lower frequencies using the covariance and correlation matrices (see Table) suggests that the two methods do not grossly differ in their sensitivity to between-condition differences in alpha "blocking."

Intracerebral Source Modeling: LORETA Analyses

Method

Data reduction. Source modeling procedures were identical to our prior report (Shackman et al., 2009). In-house code implementing the Low Resolution Brain Electromagnetic Tomography (LORETA) algorithm (Frei et al., 2001; Pascual-Marqui, 1999; Pascual-Marqui, Michel, & Lehmann, 1994) was used to model the distributed neuronal sources underlying the scalp-recorded voltage. LORETA has received more extensive cross-modal validation than alternative modeling algorithms.[2] For each participant, voxelwise current densities (A/m^2) were generated for each SFA-defined alpha sub-band using an inverse operator created using LORETA-Key (http://www.unizh.ch/keyinst/NewLORETA; $\lambda=10^{-5}$). The forward-model was comprised of a 3-shell (Ary, Klein, & Fender, 1981) head model and canonical electrode coordinates (http://www.egi.com) normalized (Towle et al., 1993) to the Montreal Neurological Institute's (MNI) probabilistic anatomical template (Collins, Neelin, Peters, & Evans, 1993) (MNI305). The source-space is restricted to the cerebral gray matter, hippocampi, and amygdalae (7-mm^3 voxels). Voxelwise source-estimates were $\log_{10}$-transformed (Thatcher, North, & Biver, 2005). Maps were exported using SPAMalize (http://brainimaging.waisman.wisc.edu/~oakes) and normalized to the MNI template (trilinear interpolation) in FLIRT (http://www.fmrib.ox.ac.uk/fsl/flirt). Final macroscopic (Duvernoy, 1999) and areal labels (Petrides, 2005) were then assigned. Our use of the term "inferior frontal junction" (IFJ) follows the convention established by Brass and colleagues (Brass, Derrfuss, Forstmann, & von Cramon, 2005).

Analytic strategy. The aim of inferential tests was to assess whether the alpha sub-bands identified using SFA differed from one another or the conventionally defined alpha bands in their sensitivity to anxious temperament, indexed by the BIS. Analyses for each band employed permutation-based nonparametric tests written in MATLAB (http://www.themathworks.com). For each, 10,000 permutations were conducted.Analyses were restricted to architectonic areas 8, 9, 10, 44, 45 and 46. The digitized atlas implemented in LORETA-Key (http://www.unizh.ch/keyinst/NewLORETA) was used to assign an architectonic label to each voxel, and the 410 voxels lying within the *a priori* region of interest (ROI) were included in analyses. A similar procedure was previously described by our laboratory (Pizzagalli, Peccoralo, Davidson, & Cohen, 2006).

Mirroring scalp analyses, intracerebral analyses relied upon voxelwise multiple regressions with BIS and BAS as simultaneous predictors of cortical current density at each voxel. Again, permutation-based nonparametric tests were employed to calculate uncorrected *p*-values. Multiple comparison correction was performed using a corrected cluster extent threshold with a preliminary intensity threshold of $p<.05$ (Nichols and Holmes, 2001). A primary threshold of uncorrected $p<.05$ was applied to the data and the volume of each contiguous cluster was recorded. Self-report data were permuted, and the volume of the largest cluster was recorded to create a distribution of maximal cluster volumes. Corrected *p*-values were calculated for each cluster on the basis of their volume using this distribution. Significance was achieved for clusters with a corrected $p<.05$.

---

[2] The validity of LORETA for modeling neural activation has been established using **(1) simulations** (Grova et al., 2006; Pascual-Marqui, Esslen, Kochi, & Lehmann, 2002; Phillips, Rugg, & Friston, 2002a, 2002b; Trujillo-Barreto, Aubert-Vazquez, & Penny, 2008; Yao & Dewald, 2005), **(2) verified epileptic foci** (Lantz et al., 1997; Worrell et al., 2000; Zumsteg, Friedman, Wennberg, & Wieser, 2005; Zumsteg, Wennberg, Treyer, Buck, & Wieser, 2005), **(3) intra-cerebral recordings** (Bai, Towle, He, & He, 2007; Seeck et al., 1998; Zumsteg, Friedman et al., 2005), **(4) positron emission tomography** (Pizzagalli et al., 2004; Zumsteg, Wennberg et al., 2005), and **(5) functional magnetic resonance imaging** (Bai et al., 2007; Corrigan et al., 2009; Duru et al., 2007; Eryilmaz, Duru, Parlak, Ademoglu, & Demiralp, 2007; Meltzer, Negishi, Mayes, & Constable, 2007; Mulert et al., 2004; Vitacco, Brandeis, Pascual-Marqui, & Martin, 2002).

Results

Because in-depth scalp and source-space analyses for the conventional alpha-low band (8-10Hz) have already been presented elsewhere (Shackman et al., 2009), we only briefly summarize key results here. In the source-space, individuals with a more anxious temperament exhibited greater activity, indexed by a reduction in alpha band current density (A/m^2), in a right dorsolateral prefrontal cortex (dlPFC) cluster lying predominantly in the right posterior middle frontal gyrus and inferior frontal gyrus pars opercularis in the vicinity of the IFJ (areas 9/46v, 8Av, 44; corrected cluster *ps*<0.05). Cluster volume differed somewhat across bands (39-27 voxels). The largest clusters were associated with the conventional alpha and alpha-low bands. The somewhat smaller clusters associated with the remaining sub-bands were always contained within this volume. Peak relations between individual differences in BIS and right dlPFC activity were similar across alpha bands, *r*s = -.32 to -.37, *p*s < .05 (corrected). Differences across bands were not significant, *p*s > .64. For the conventional alpha and alpha-low bands the peak fell in right posterior dlPFC (right-pdlPFC; 53,24,29; area 9/46v; uncorrected peak *p*=0.003). Peak locations for the remaining bands were similar, falling within 2 voxels of this location (Euclidean displacement < 9.9 mm). The conventional alpha-high band was associated with the smallest cluster and weakest correlation, *r* = -.32.

Supplementary References

Arruda, J. E., Weiler, M. D., Valentino, D., Willis, W. G., Rossi, J. S., Stern, R. A., et al. (1996). A guide for applying principal-components analysis and confirmatory factor analysis to quantitative electroencephalogram data. *International Journal of Psychophysiology, 23*, 63-81.

Ary, J. P., Klein, S. A., & Fender, D. H. (1981). Location of sources of evoked scalp potentials: corrections for skull and scalp thicknesses. *IEEE Transactions on Biomedical Engineering, 28*, 447-452.

Babiloni, C., Cassetta, E., Binetti, G., Tombini, M., Del Percio, C., Ferreri, F., et al. (2007). Resting EEG sources correlate with attentional span in mild cognitive impairment and Alzheimer's disease. *European Journal of Neuroscience, 25*, 3742-3757.

Bai, X., Towle, V. L., He, E. J., & He, B. (2007). Evaluation of cortical current density imaging methods using intracranial electrocorticograms and functional MRI. *Neuroimage, 35*, 598-608.

Bernat, E. M., Williams, W. J., & Gehring, W. J. (2005). Decomposing ERP time-frequency energy using PCA. *Clinical Neurophysiology, 116*, 1314-1334.

Brass, M., Derrfuss, J., Forstmann, B., & von Cramon, D. Y. (2005). The role of the inferior frontal junction in cognitive control. *Trends in Cognitive Sciences, 9*, 314-316.

Cacace, A. T., & McFarland, D. J. (2003). Quantifying signal-to-noise ratio of mismatch negativity in humans. *Neuroscience Letters, 341*, 251-255.

Carver, C. S., & White, T. L. (1994). Behavioral inhibition, behavioral activation, and affective responses to impending reward and punishment: The BIS/BAS Scales. *Journal of Personality and Social Psychology, 67*, 319-333.

Chapman, L. J., & Chapman, J. P. (1973). Problems in the measurement of cognitive deficits. *Psychological Bulletin, 79*, 380-385.

Chapman, L. J., & Chapman, J. P. (1978). The measurement of differential deficit. *Journal of Psychiatric Research, 14*, 303-311.

Chapman, L. J., & Chapman, J. P. (2001). Commentary on two articles concerning generalized and specific cognitive deficits. *Journal of Abnormal Psychology, 110*, 31-39.

Clark, L. A., & Watson, D. (1995). Constructing validity: Basic issues in objective scale development. *Psychological Assessment, 7*, 309-319.

Coan, J. A., & Allen, J. J. B. (2004). Frontal EEG asymmetry as a moderator and mediator of emotion. *Biological Psychology, 67*, 7-49.

Collins, D. L., Neelin, P., Peters, T. M., & Evans, A. C. (1993). Automatic 3D intersubject registration of MR volumetric data in standardized Talairach space. *Journal of Computer Assisted Tomography, 18*, 192-205.

Comrey, A. L., & Lee, H. B. (1992). *A first course in factor analysis* (2nd ed.). Hillsdale, NJ: LEA.

Corrigan, N. M., Richards, T., Webb, S. J., Murias, M., Merkle, K., Kleinhans, N. M., et al. (2009). An investigation of the relationship between fMRI and ERP source localized measurements of brain activity during face processing. *Brain Topography, 22*, 83-96.

Cronbach, L. J. (1960). *Essentials of psychological testing* (2nd ed.). NY: Harper & Row.

Cronbach, L. J., & Meehl, P. E. (1955). Construct validity in psychological tests. *Psychological Bulletin, 52*, 281-302.

Davidson, R. J., Chapman, J. P., Chapman, L. J., & Henriques, J. B. (1990). Asymmetrical brain electrical activity discriminates between psychometrically-matched verbal and spatial cognitive tasks. *Psychophysiology, 27*, 528-543.

Dien, J. (*in press-a*). The ERP PCA Toolkit: An open source program for advanced statistical analysis of event-related potential data. *Journal of Neuroscience Methods*.

Dien, J. (*in press-b*). Evaluating two-step PCA of ERP data with geomin, infomax, oblimin, promax, and varimax rotations. *Psychophysiology*.

Donchin, E., & Heffley, E. (1978). Multivariate analysis of event-related potential data: A tutorial review. In D. A. Otto (Ed.), *Multidisciplinary perspectives in event-related brain potential research* (pp. 555-572). Washington, DC: US Environmental Protection Agency Office of Research and Development.

Duru, A. D., Eryilmaz, H., Emir, U., Bayraktaroglu, Z., Demiralp, T., & Ademoglu, A. (2007). Implementation of low resolution electro-magnetic tomography with FMRI statistical maps on realistic head models. *Conf Proc IEEE Eng Med Biol Soc, 2007*, 5239-5242.

Duvernoy, H. M. (1999). *The human brain. Surface, Three-dimensional sectional anatomy with MRI, and blood supply* (2nd ed.). NY: Springer.

Eryilmaz, H. H., Duru, A. D., Parlak, B., Ademoglu, A., & Demiralp, T. (2007). Neuroimaging of event related brain potentials (ERP) using fMRI and dipole source reconstruction. *Conf Proc IEEE Eng Med Biol Soc, 2007*, 3384-3387.

Fava, J. L., & Velicer, W. F. (1992). An empirical comparison of factor, image, component, and scale scores. *Multivariate Behavioral Research, 27*, 301-322.

Fava, J. L., & Velicer, W. F. (1996). The effects of underextraction in factor and component analysis. *Educational and Psychological Measurement, 56*, 907-929.

Feldt, L. S., Woodruff, D. J., & Salih, F. A. (1987). Statistical inference for coeeficient alpha. *Applied Psychological Measurement, 11*, 93-103.

Ferree, T. C., Brier, M. R., Hart, J., Jr., & Kraut, M. A. (2009). Space-time-frequency analysis of EEG data using within-subject statistical tests followed by sequential PCA. *Neuroimage, 45*, 109-121.

Floyd, F. J., & Widaman, K. F. (1995). Factor analysis in the development and refinement of clinical assessment instruments. *Psychological Assessment, 7*, 286-299.

Frei, E., Gamma, A., Pascual-Marqui, R., Lehmann, D., Hell, D., & Vollenweider, F. X. (2001). Localization of MDMA-induced brain activity in healthy volunteers using low resolution brain electromagnetic tomography (LORETA). *Human Brain Mapping, 14*, 152-165.

Gorsuch, R. L. (1983). *Factor analysis* (2nd ed.). Hillsdale, NJ: LEA.

Guilford, J. P. (1954). *Psychometric methods* (2nd ed.). NY: McGraw-Hill.

Handy, T. C. (2005). Basic principles of ERP quantification. In T. C. Handy (Ed.), *Evoked potentials: a methods handbook* (pp. 33-56). Cambridge, MA: MIT Press.

Harman, H. H. (1976). *Modern factor analysis* (3rd ed.). Chicago: University of Chicago Press.

Hogan, J., & Roberts, B. W. (1996). Issues and non-issues in the fidelity-bandwidth trade-off. *Journal of Organizational Behavior, 17*, 627-637.

Huettel, S. A., Singerman, J. D., & McCarthy, G. (2001). The effects of aging upon the hemodynamic response measured by functional MRI. *Neuroimage, 13*, 161-175.

Kayser, J., & Tenke, C. E. (2006). Consensus on PCA for ERP data, and sensibility of unrestricted solutions. *Clinical Neurophysiology, 117*, 703-707.

Lantz, G., Michel, C. M., Pascual-Marqui, R. D., Spinelli, L., Seeck, M., Seri, S., et al. (1997). Extracranial localization of intracranial interictal epileptiform activity using LORETA (low resolution electromagnetic tomography). *Electroencephalography and Clinical Neurophysiology, 102*, 414-422.

Lawrence, F. R., & Hancock, G. R. (1999). Conditions affecting integrity of a factor solution under varying degrees of overextraction. *Educational and Psychological Measurement, 59*, 549-579.

Lee, H., Shackman, A. J., Jackson, D. C., & Davidson, R. J. (2009). Test-retest reliability of voluntary emotion regulation. *Psychophysiology, 46*, 874-879.

Loevinger, J. (1957). Objective tests as instruments of psychological theory. *Psychological Reports, 3*, 635-694.

Luck, S. J. (2005). *An introduction to the event-related potential technique*. Cambridge, MA: MIT Press.

Maltez, J., Hyllienmark, L., Nikulin, V. V., & Brismar, T. (2004). Time course and variability of power in different frequency bands of EEG during resting conditions. *Neurophysiologie Clinique, 34*, 195-202.

Melinder, M. R., Barch, D. M., Heydebrand, G., & Csernansky, J. G. (2005). Easier tasks can have better discriminating power: the case of verbal fluency. *Journal of Abnormal Psychology, 114*, 385-391.

Meltzer, J. A., Negishi, M., Mayes, L. C., & Constable, R. T. (2007). Individual differences in EEG theta and alpha dynamics during working memory correlate with fMRI responses across subjects. *Clinical Neurophysiology, 118*, 2419-2436.

Mocks, J., Gasser, T., & Kohler, W. (1988). Basic statistical parameters of event-related potentials. *Journal of Psychophysiology, 2*.

Mulert, C., Jager, L., Schmitt, R., Bussfeld, P., Pogarell, O., Moller, H. J., et al. (2004). Integration of fMRI and simultaneous EEG: towards a comprehensive understanding of localization and time-course of brain activity in target detection. *Neuroimage, 22*, 83-94.

Nunnally, J. C., & Bernstein, I. H. (1994). *Psychometric theory* (3rd ed.). NY: McGraw-Hill.

Parrish, T. B., Gitelman, D. R., LaBar, K. S., & Mesulam, M. M. (2000). Impact of signal-to-noise on functional MRI. *Magnetic Resonance in Medicine, 44*, 925-932.

Pascual-Marqui, R. D. (1999). Review of methods for solving the EEG inverse problem. *International Journal of Bioelectromagnetism, 1*, 75-86.

Pascual-Marqui, R. D., Michel, C. M., & Lehmann, D. (1994). Low resolution electromagnetic tomography: a new method for localizing electrical activity in the brain. *International Journal of Psychophysiology, 18*, 49-65.

Petrides, M. (2005). Lateral prefrontal cortex: architectonic and functional organization. *Philosophical Transactions of the Royal Society of London. Series B, 360*, 781-795.

Pizzagalli, D. A., Oakes, T. R., Fox, A. S., Chung, M. K., Larson, C. L., Abercrombie, H. C., et al. (2004). Functional but not structural subgenual prefrontal cortex abnormalities in melancholia. *Molecular Psychiatry, 9*, 325, 393-405.

Pizzagalli, D. A., Peccoralo, L. A., Davidson, R. J., & Cohen, J. D. (2006). Resting anterior cingulate activity and abnormal responses to errors in subjects with elevated depressive symptoms: A 128-Channel EEG study. *Human Brain Mapping, 27*, 185-201.

Rosenthal, R., & Rosnow, R. L. (1991). *Essentials of behavioral research: Methods and data analysis* (2nd ed.). NY: McGraw-Hill.

Seeck, M., Lazeyras, F., Michel, C. M., Blanke, O., Gericke, C. A., Ives, J., et al. (1998). Non-invasive epileptic focus localization using EEG-triggered functional MRI and electromagnetic tomography. *Electroencephalography and Clinical Neurophysiology, 106*, 508-512.

Shackman, A. J., McMenamin, B. W., Maxwell, J. S., Greischar, L. L., & Davidson, R. J. (2009). Right dorsolateral prefrontal cortical activity and behavioral inhibition. *Psychological Science, 20*, 1500-1506.

Shackman, A. J., Sarinopoulos, I., Maxwell, J. S., Pizzagalli, D. A., Lavric, A., & Davidson, R. J. (2006). Anxiety selectively disrupts visuospatial working memory. *Emotion, 6*, 40-61.

Strube, M. J., & Newman, L. C. (2007). Psychometrics. In J. T. Cacioppo, L. G. Tassinary & G. G. Berntson (Eds.), *Handbook of psychophysiology* (3rd ed., pp. 789-811). NY: Cambridge University Press.

Thatcher, R. W., North, D., & Biver, C. (2005). Parametric vs. non-parametric statistics of low resolution electromagnetic tomography (LORETA). *Clinical EEG and Neuroscience, 36*, 1-8.

Tomarken, A. J., Davidson, R. J., Wheeler, R. E., & Kinney, L. (1992). Psychometric properties of resting anterior EEG asymmetry: Temporal stability and internal consistency. *Psychophysiology, 29*, 576-592.

Towers, D. N., & Allen, J. J. B. (2009). A better estimate of the internal consistency reliability of frontal EEG asymmetry scores. *Psychophysiology, 46*, 132-142.

Towle, V. L., Bolanos, J., Suarez, D., Tan, K., Grzeszczuk, R., Levin, D. N., et al. (1993). The spatial location of EEG electrodes: locating the best-fitting sphere relative to cortical anatomy. *Electroencephalography and Clinical Neurophysiology, 86*, 1-6.

Van Albada, S. J., Rennie, C. J., & Robinson, P. A. (2007). Variability of model-free and model-based quantitative measures of EEG. *Journal of Integrative Neuroscience, 6*, 279-307.

Vitacco, D., Brandeis, D., Pascual-Marqui, R., & Martin, E. (2002). Correspondence of event-related potential tomography and functional magnetic resonance imaging during language processing. *Human Brain Mapping, 17*, 4-12.

Wood, J. M., Tataryn, D. J., & Gorsuch, R. L. (1996). Effects of under- and overextraction on pricipal axis factor analysis with varimax rotation. *Psychological Methods, 1*, 354-365.

Worrell, G. A., Lagerlund, T. D., Sharbrough, F. W., Brinkmann, B. H., Busacker, N. E., Cicora, K. M., et al. (2000). Localization of the epileptic focus by low-resolution electromagnetic tomography in patients with a lesion demonstrated by MRI. *Brain Topography, 12*, 273-282.

Zimmerman, D. W., & Williams, R. H. (1986). Note on the reliability of experimental measures and the power of significance tests. *Psychological Bulletin, 100*, 123-124.

Zimmerman, D. W., Williams, R. H., & Zumbo, B. D. (1993). Reliability of measurement and power of significance tests based on differences. *Applied Psychological Measurement, 17*, 1-9.

Zumsteg, D., Friedman, A., Wennberg, R. A., & Wieser, H. G. (2005). Source localization of mesial temporal interictal epileptiform discharges: correlation with intracranial foramen ovale electrode recordings. *Clinical Neurophysiology, 116*, 2810-2818.

Zumsteg, D., Wennberg, R. A., Treyer, V., Buck, A., & Wieser, H. G. (2005). H2(15)O or 13NH3 PET and electromagnetic tomography (LORETA) during partial status epilepticus. *Neurology, 65*, 1657-1660.

Zwick, W. R., & Velicer, W. F. (1986). Comparison of five rules for determing the number of components to retain. *Psychological Bulletin, 99*, 432-442.